COLLAGE 2019

Large-Scale Solar Magnetic Fields

Xudong Sun (UH/IfA)

Apr 02 2019

Outline

- Solar features & magnetic origin
- Photospheric magnetic field maps
- Potential field model of quiescent corona

Solar Feature & Magnetic Origin

A Steep Stratification

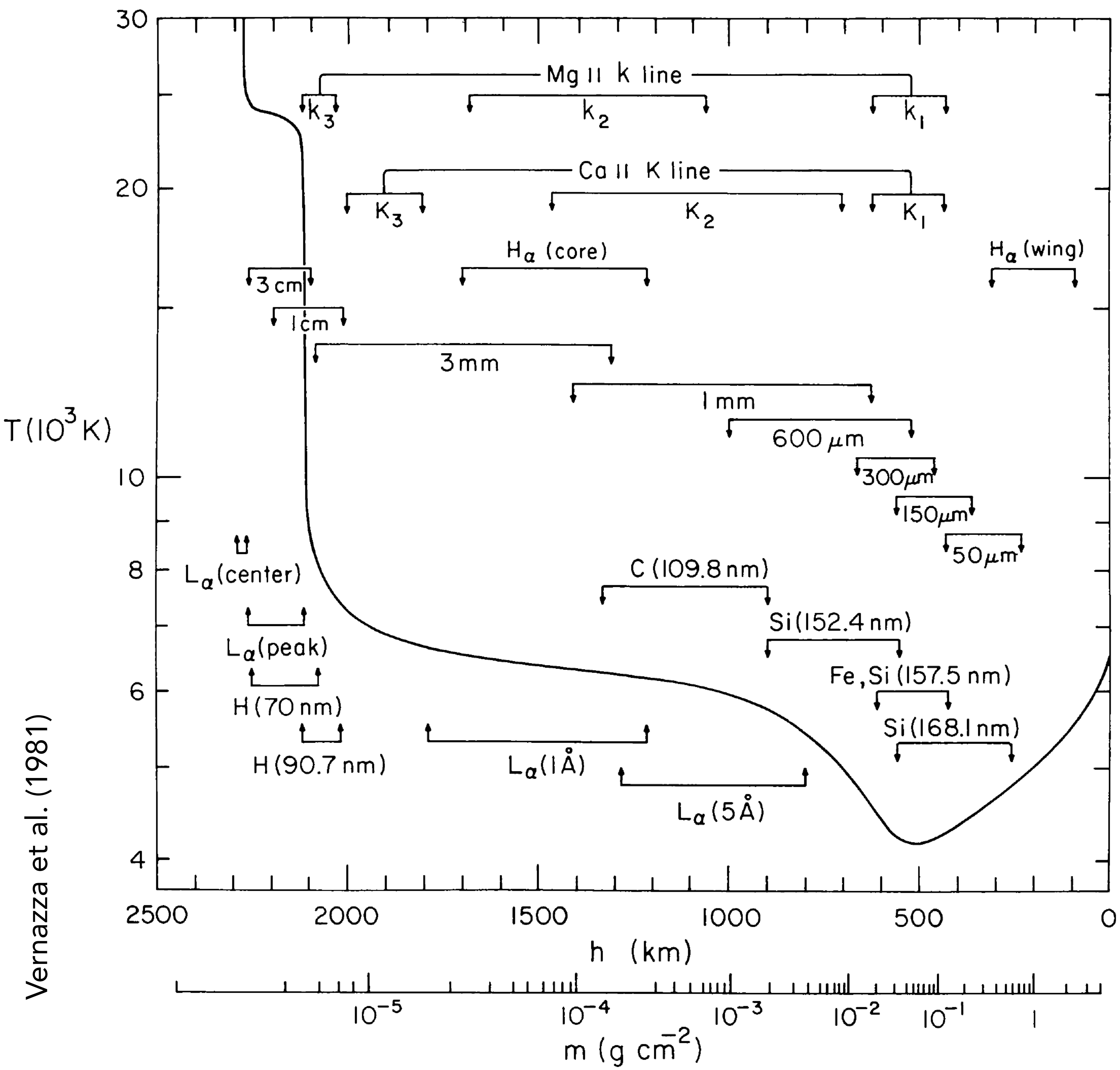

Vernazza et al. (1981)

- Different spectral lines probe different "layers" of solar atmosphere
- Large contrast in spatial and temporal scales
- Rich information resides in specto-polarization signals as well as emission morphology

The Multi-Wavelength Sun

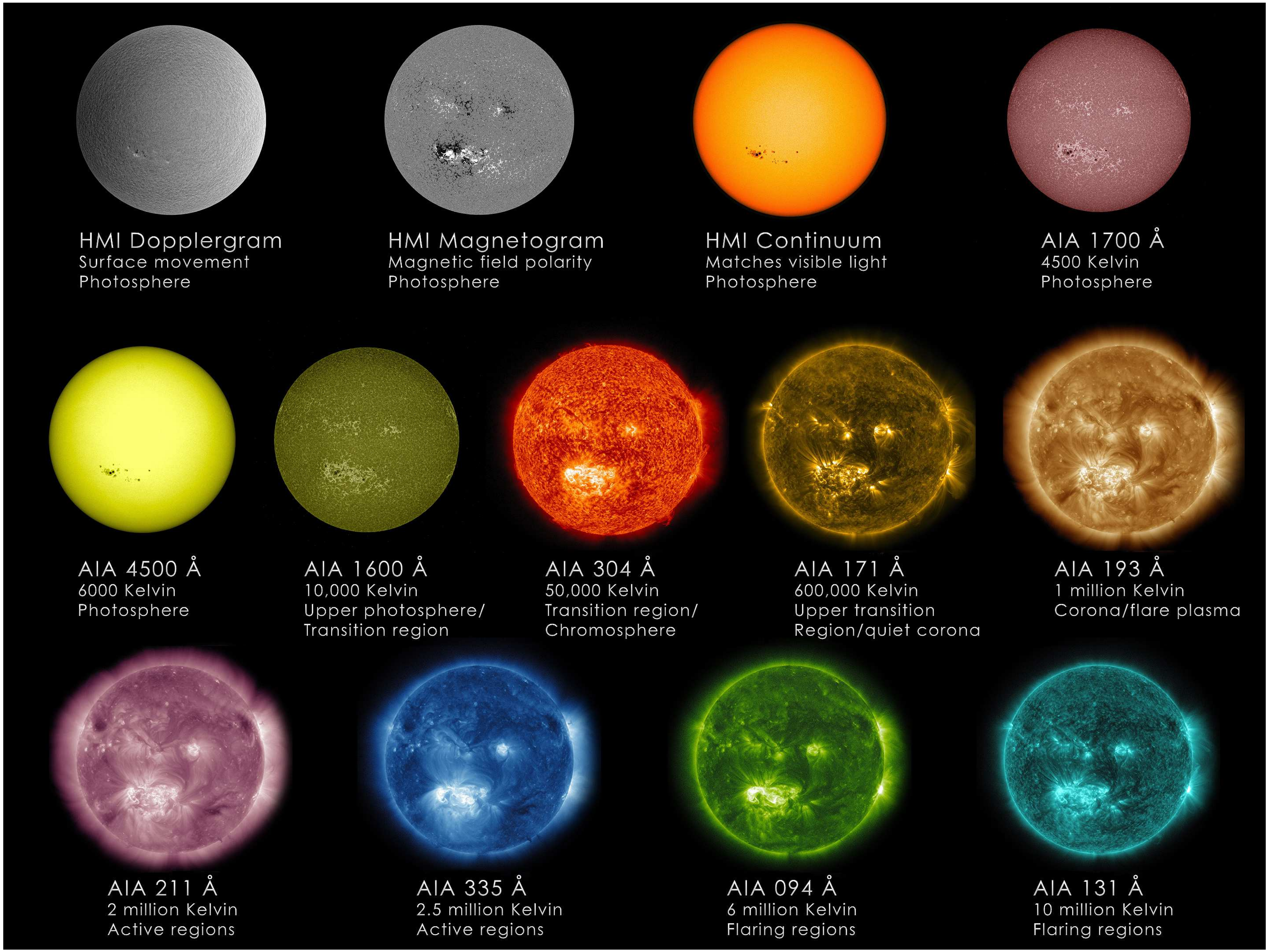

Photosphere: Full Disk View

SDO/HMI Fe I 617.3 nm; 1″ resolution

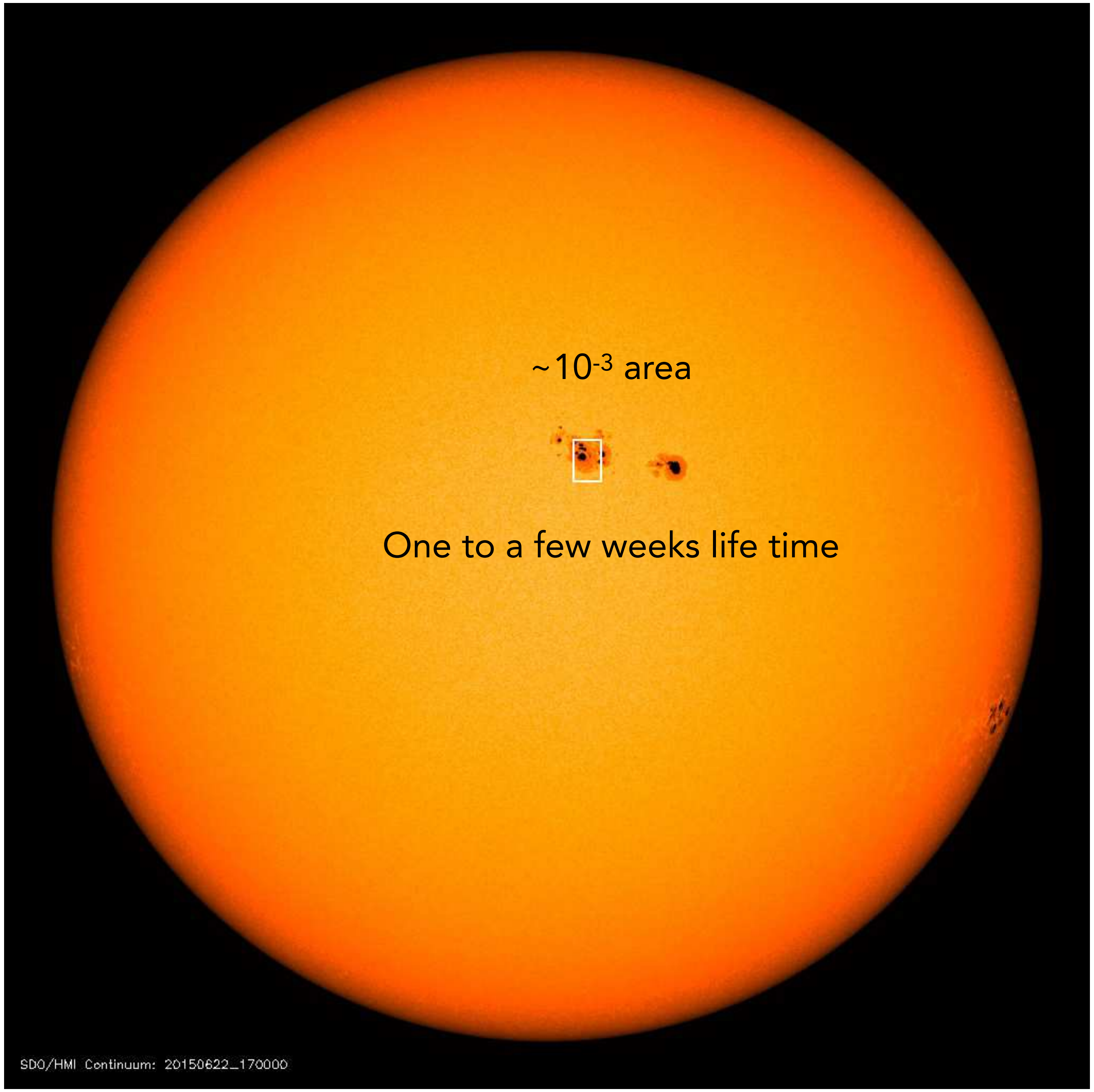

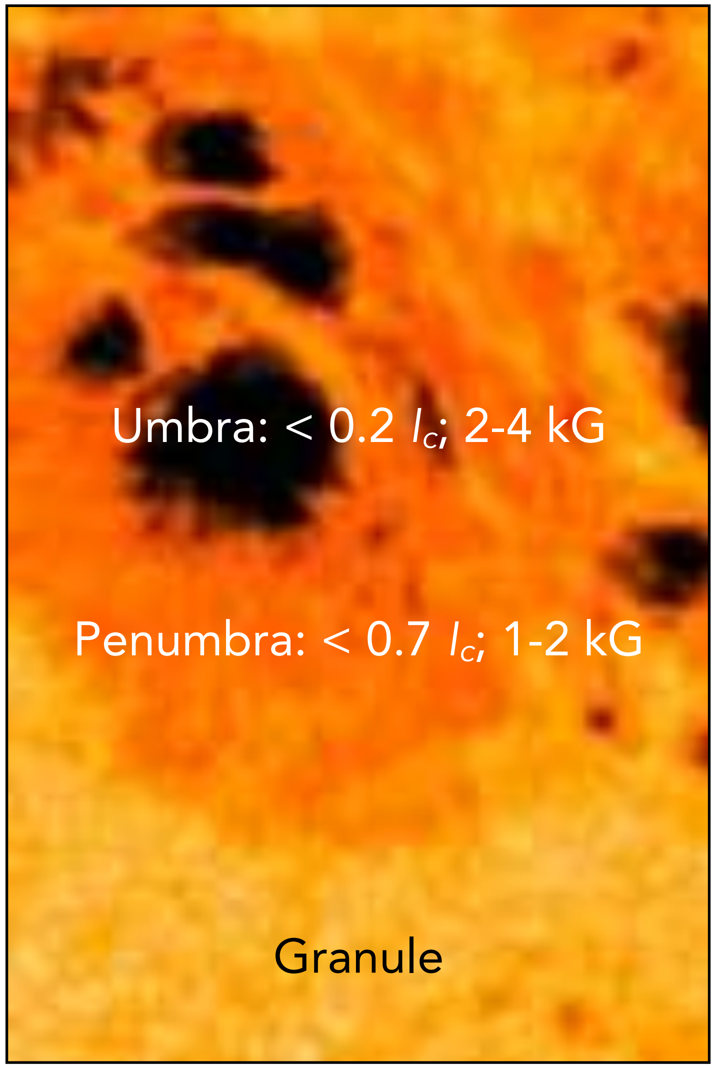

Photosphere: High Resolution

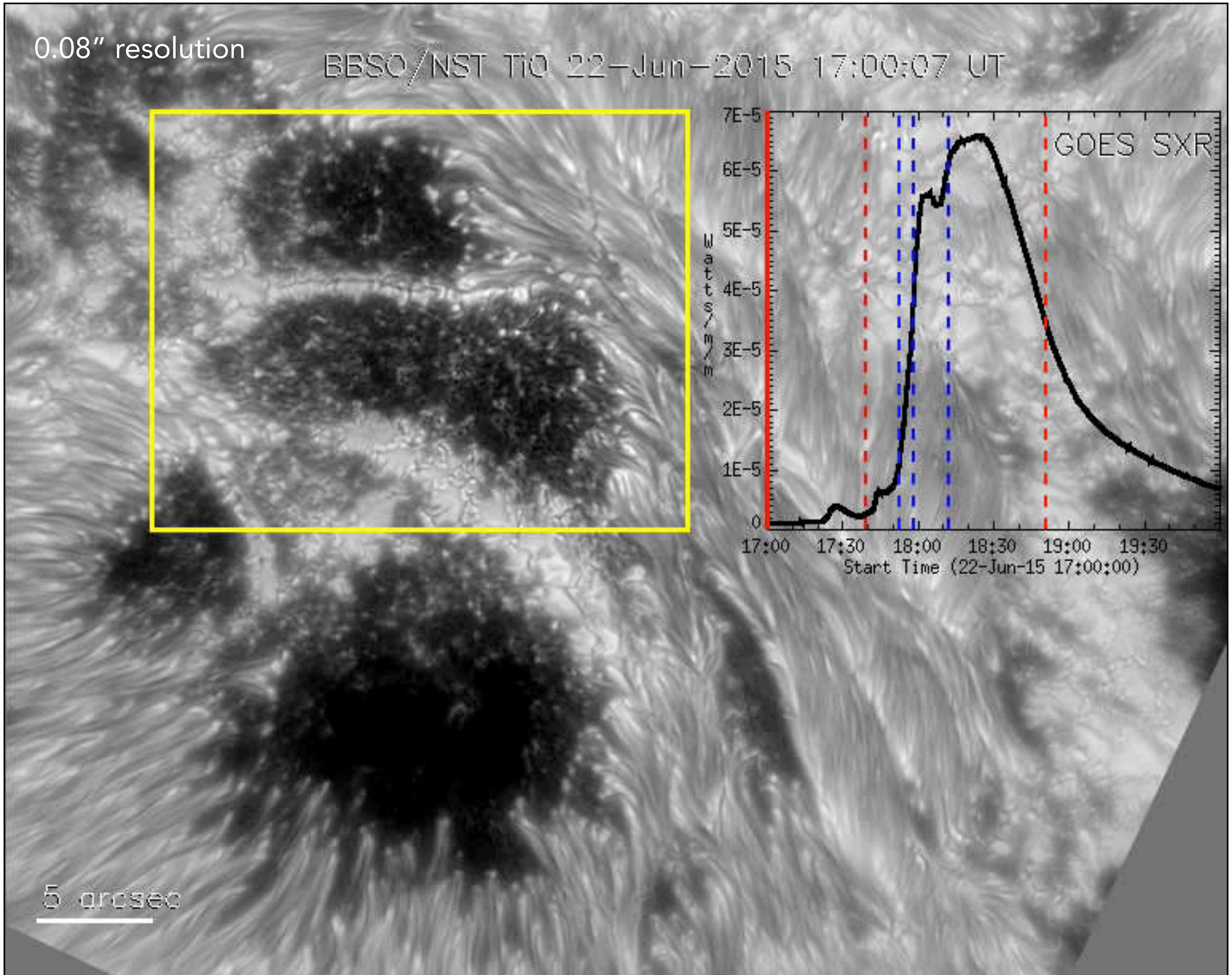

Liu et al. (2016)

Chromosphere: On Disk

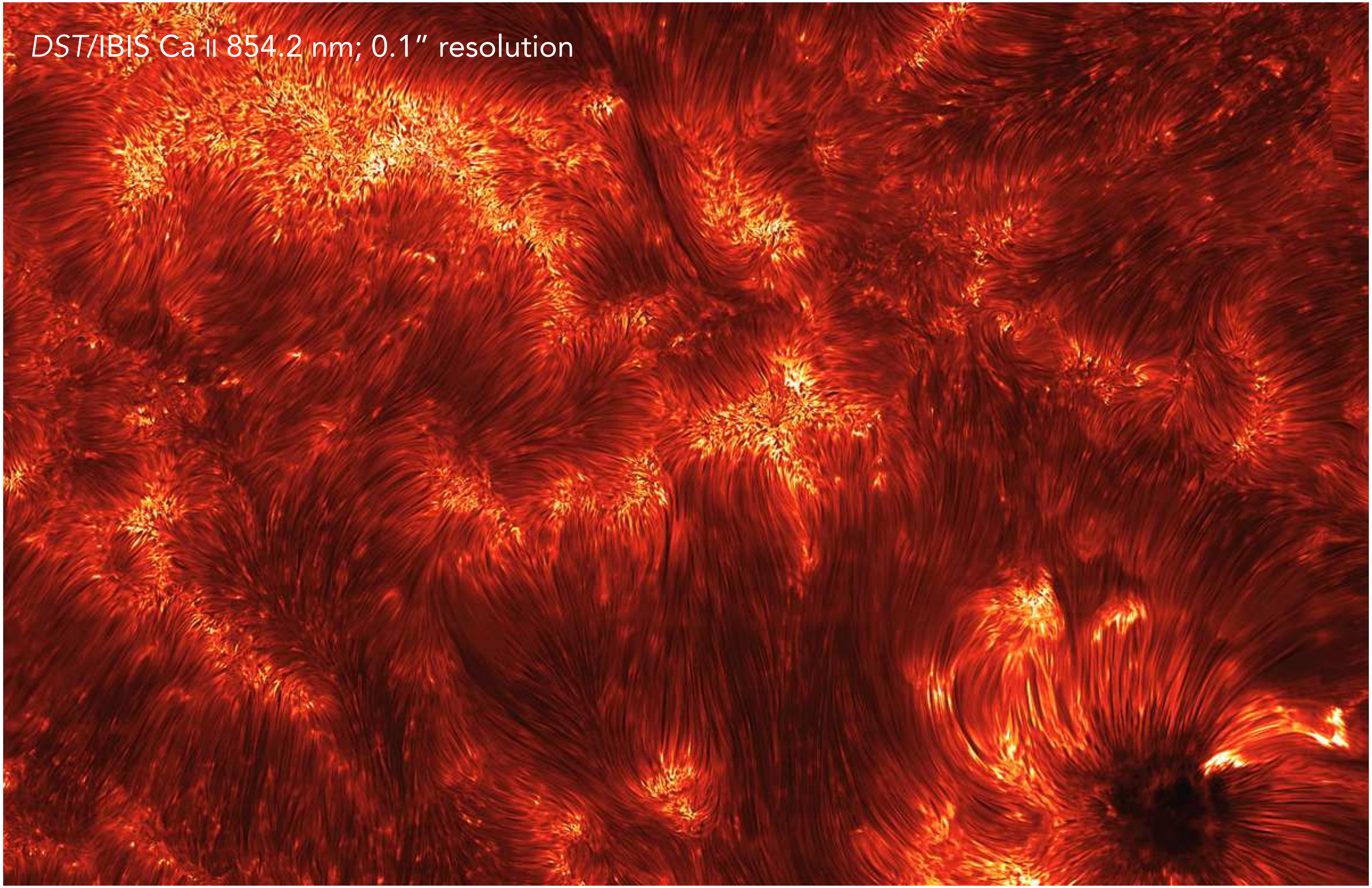

Reardon et al. (2011)

Chromosphere: Off Limb

Hinode/SOT Ca II H line 396.9 nm; 0.2” resolution

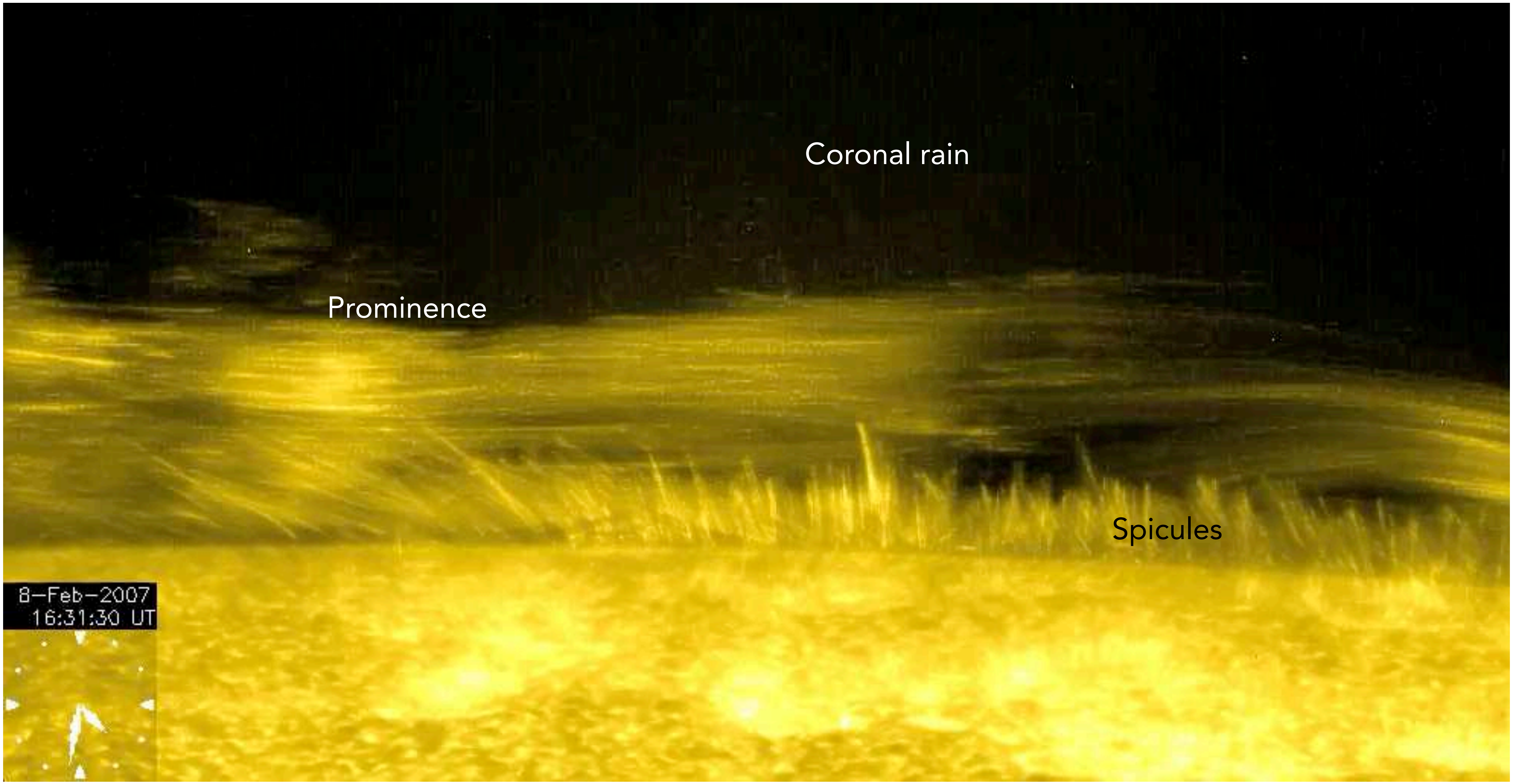

Okamoto et al. (2016)

Magnetic Connectivity: Sunspot

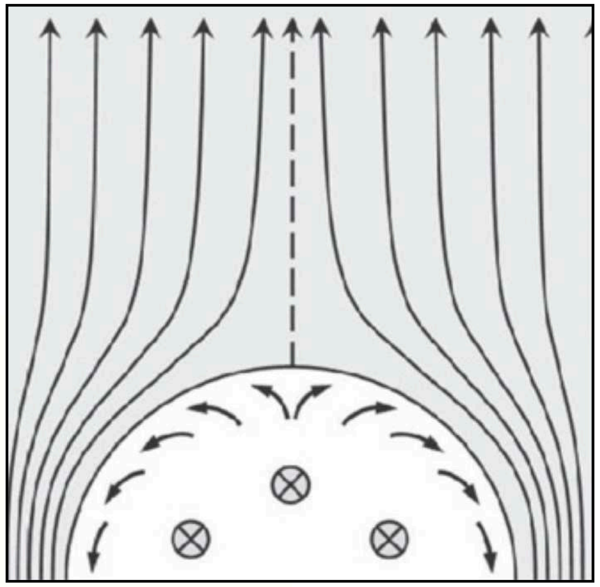

Zakharov et al. (2008)
Rempel et al. (2009)

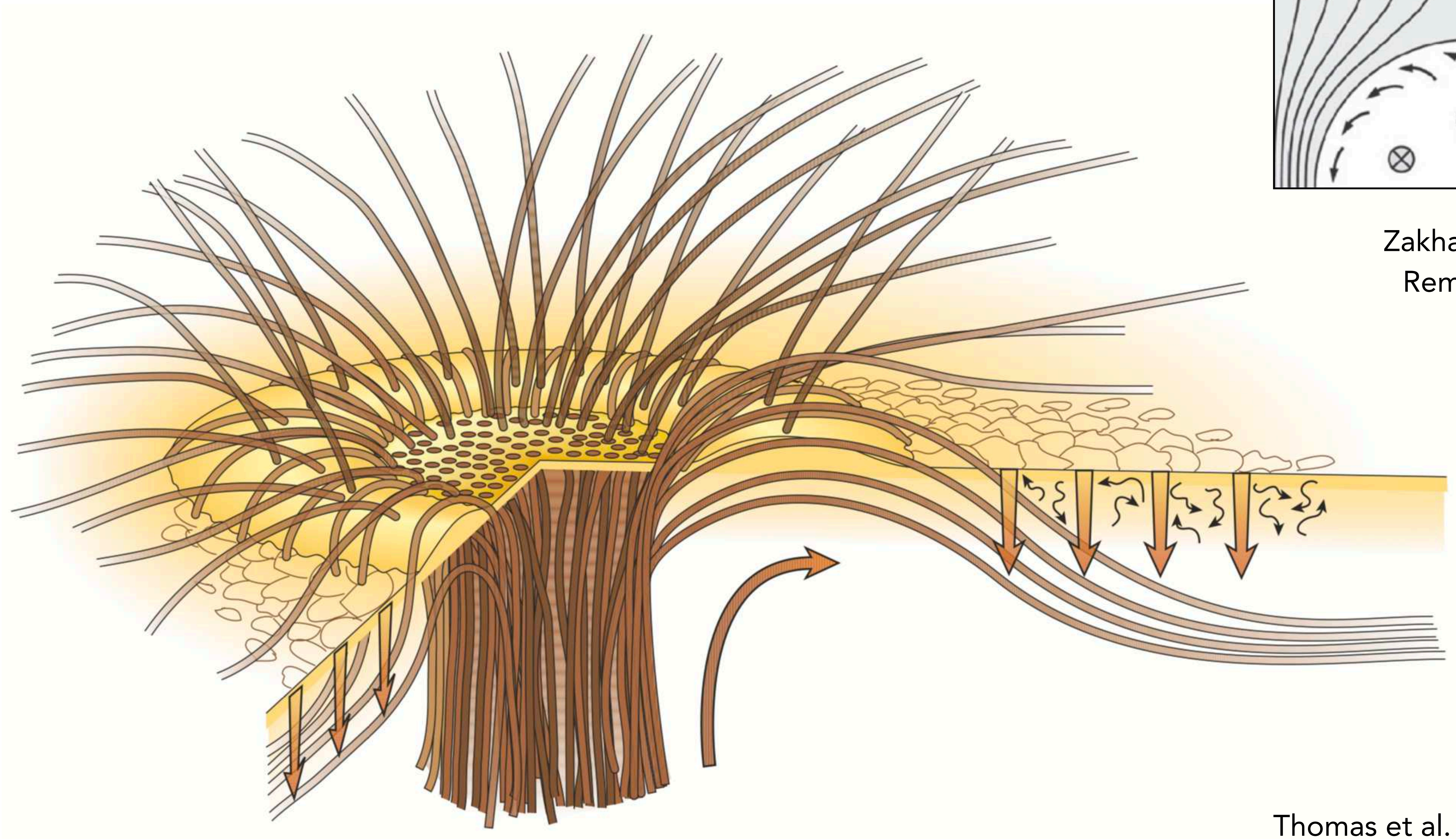

Thomas et al. (2002)

Magnetic Connectivity: Quiet Sun

Wedemeyer-Böhm et al. (2008)

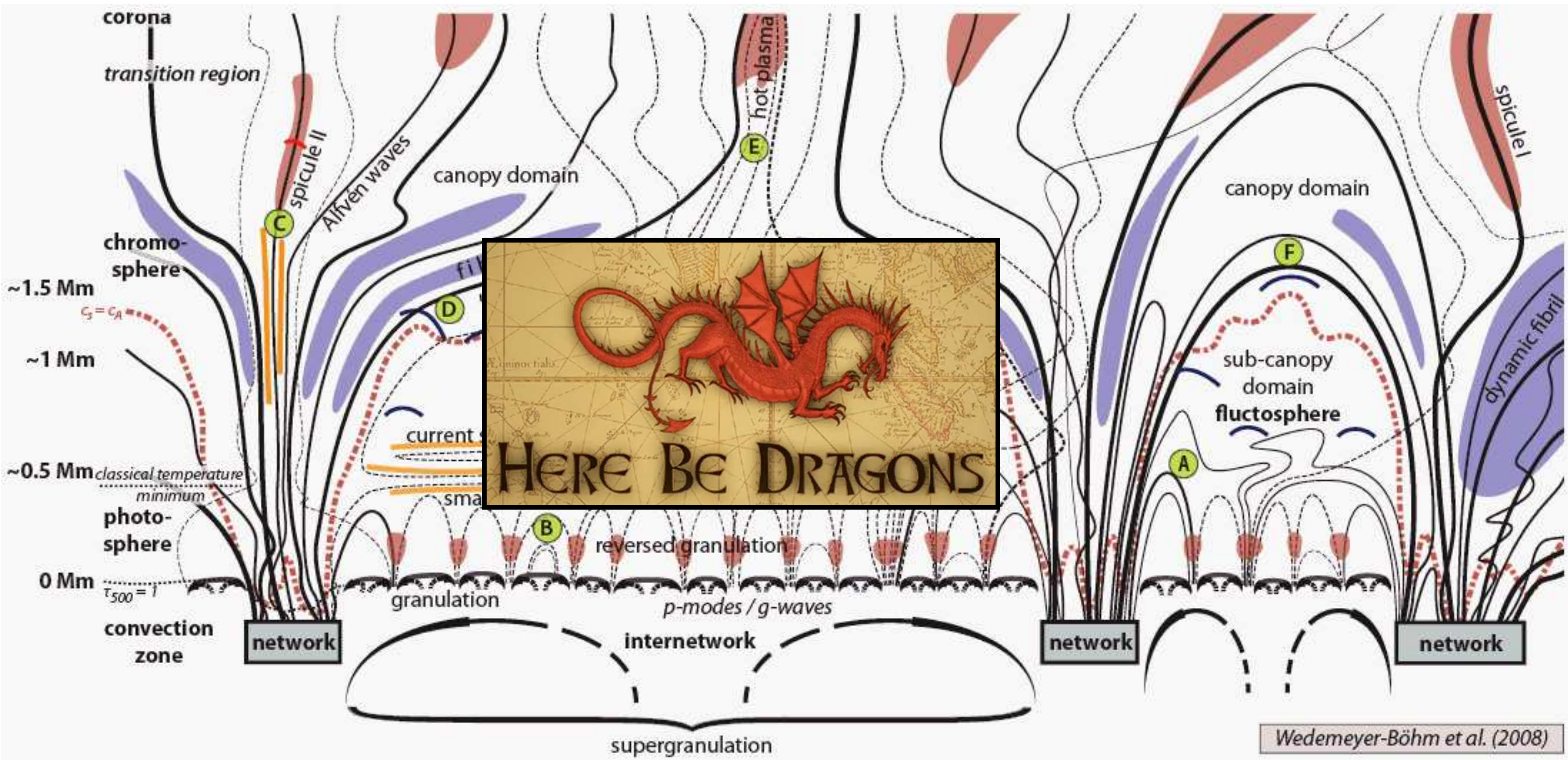

When drawn to scale

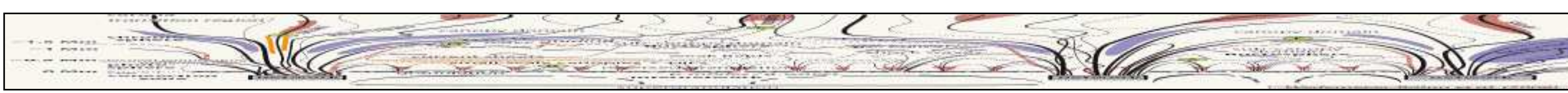

Corona: Active Region Loop

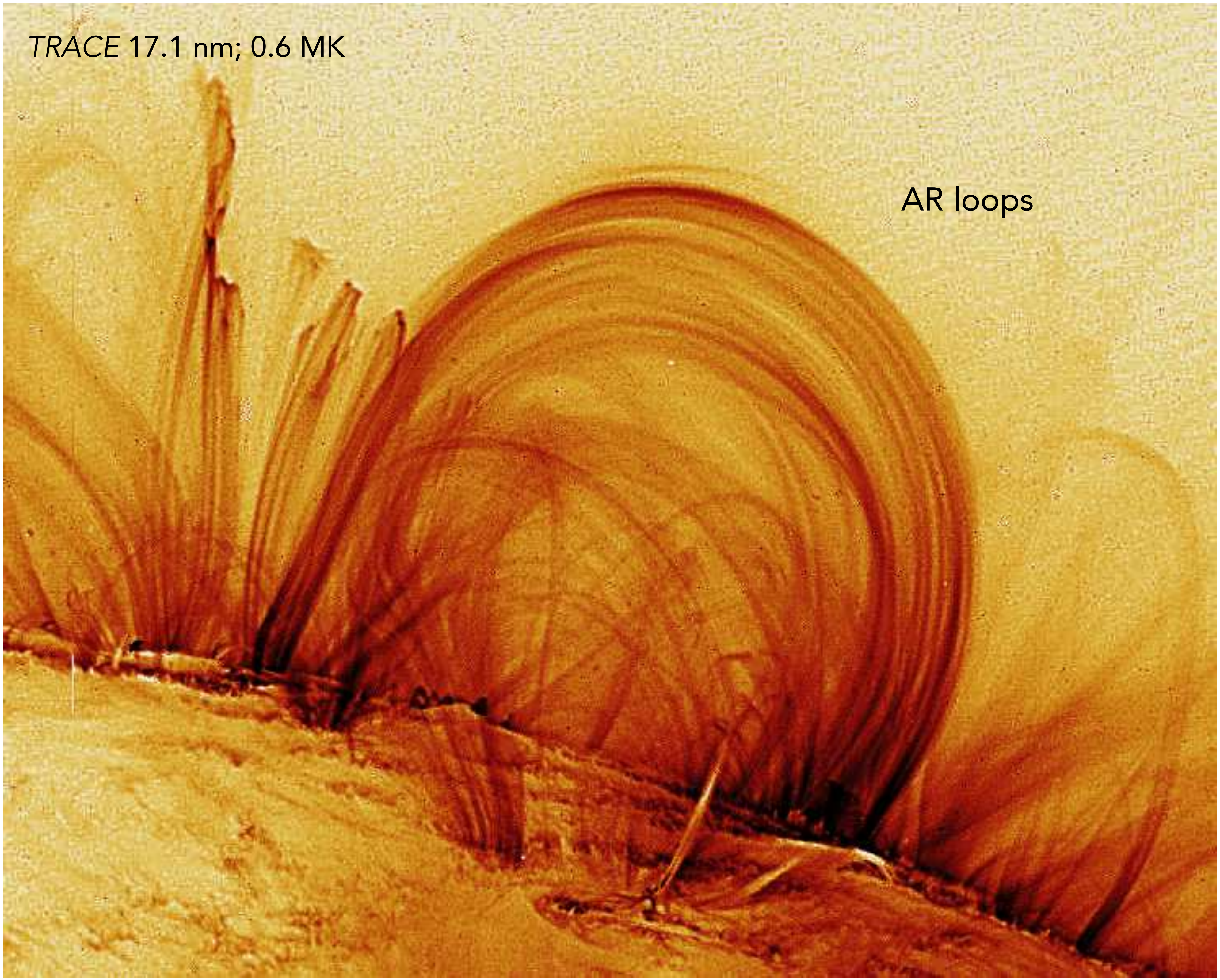

Corona: Coronal Hole

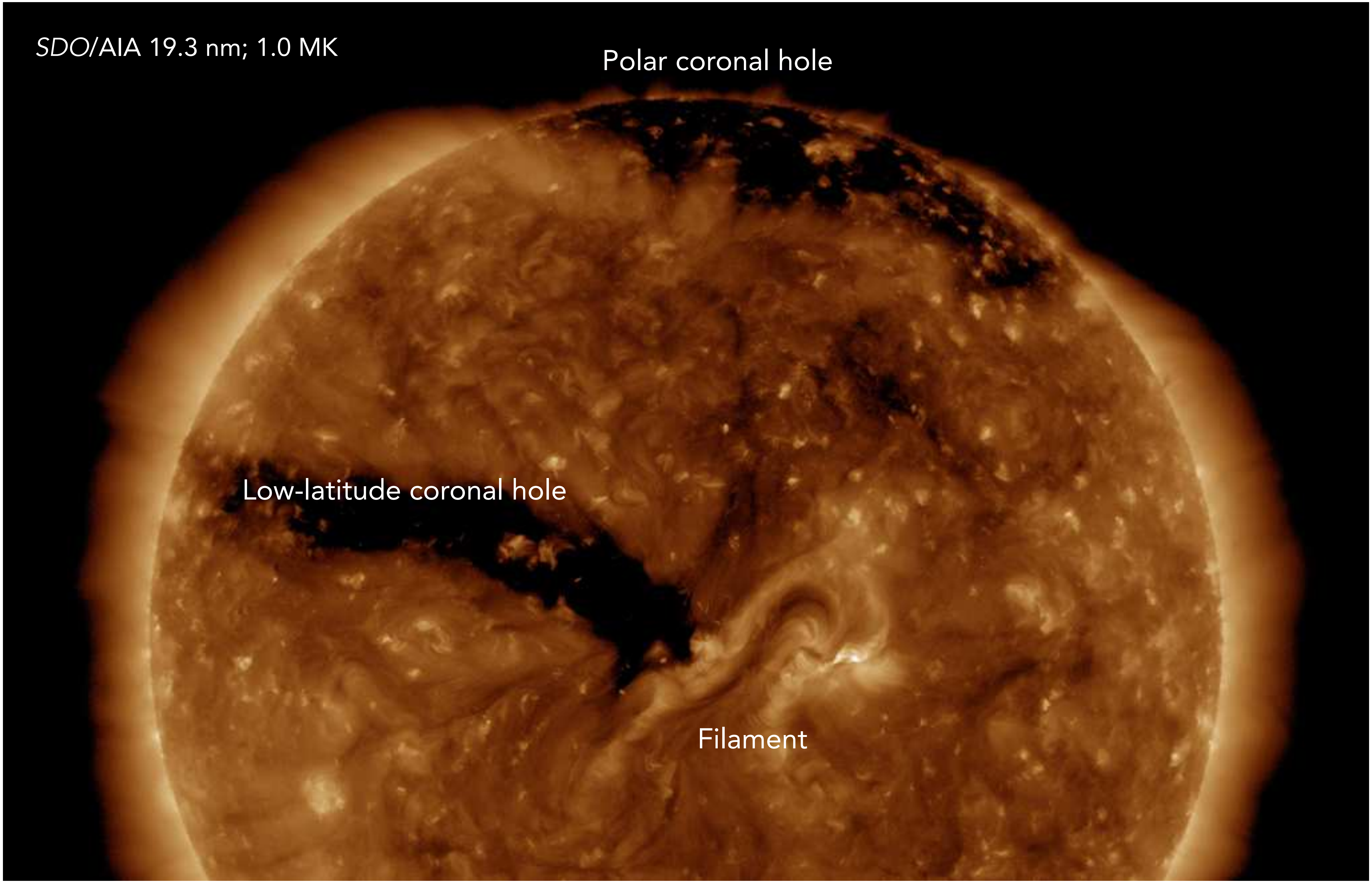

Magnetic Connectivity: Cartoon

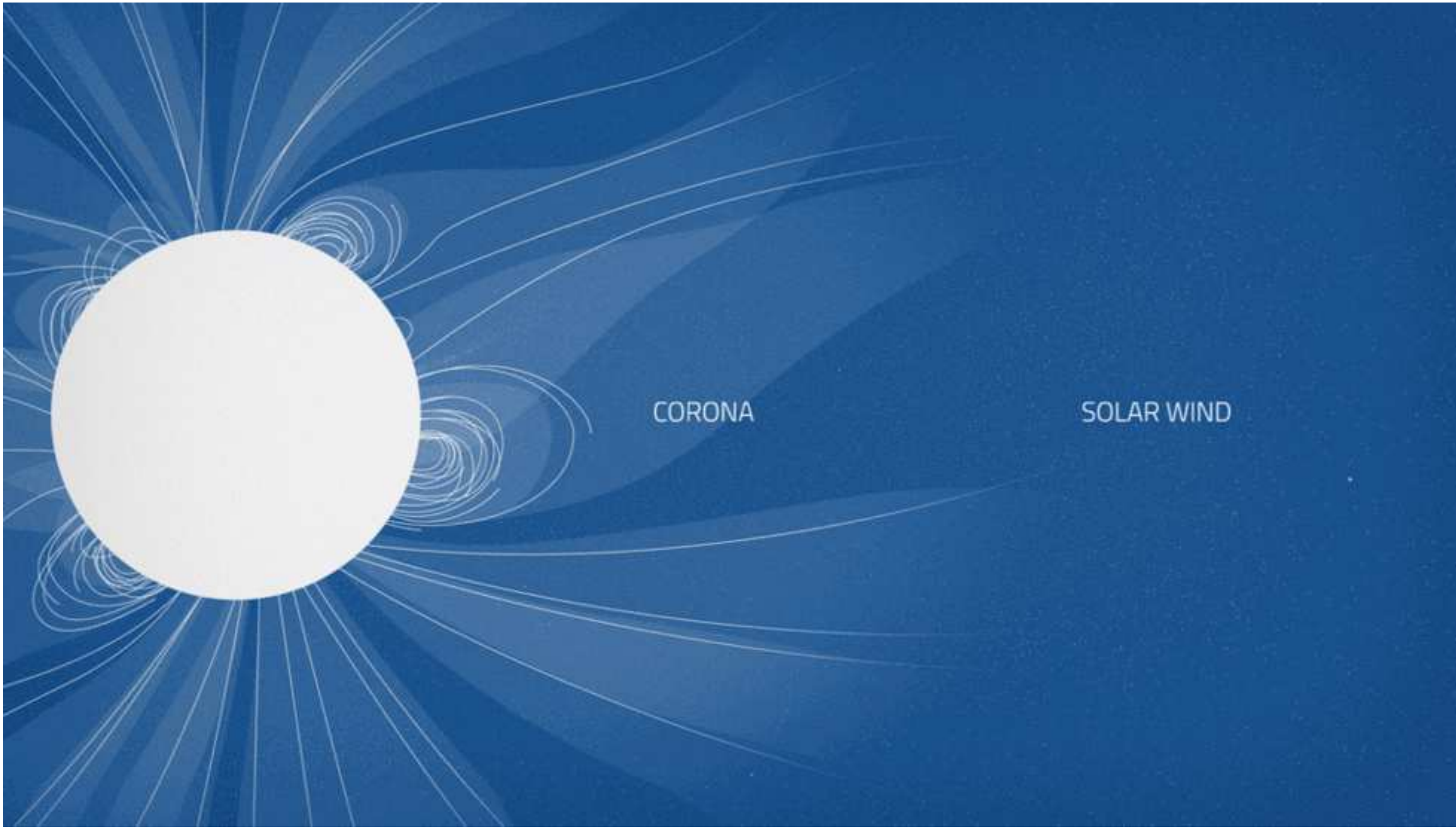

https://spaceplace.nasa.gov/sun-corona/en/

Magnetic Connectivity: Model

Mikić et al. (2018)

Magnetic Connectivity: Heliosphere

Parker spiral

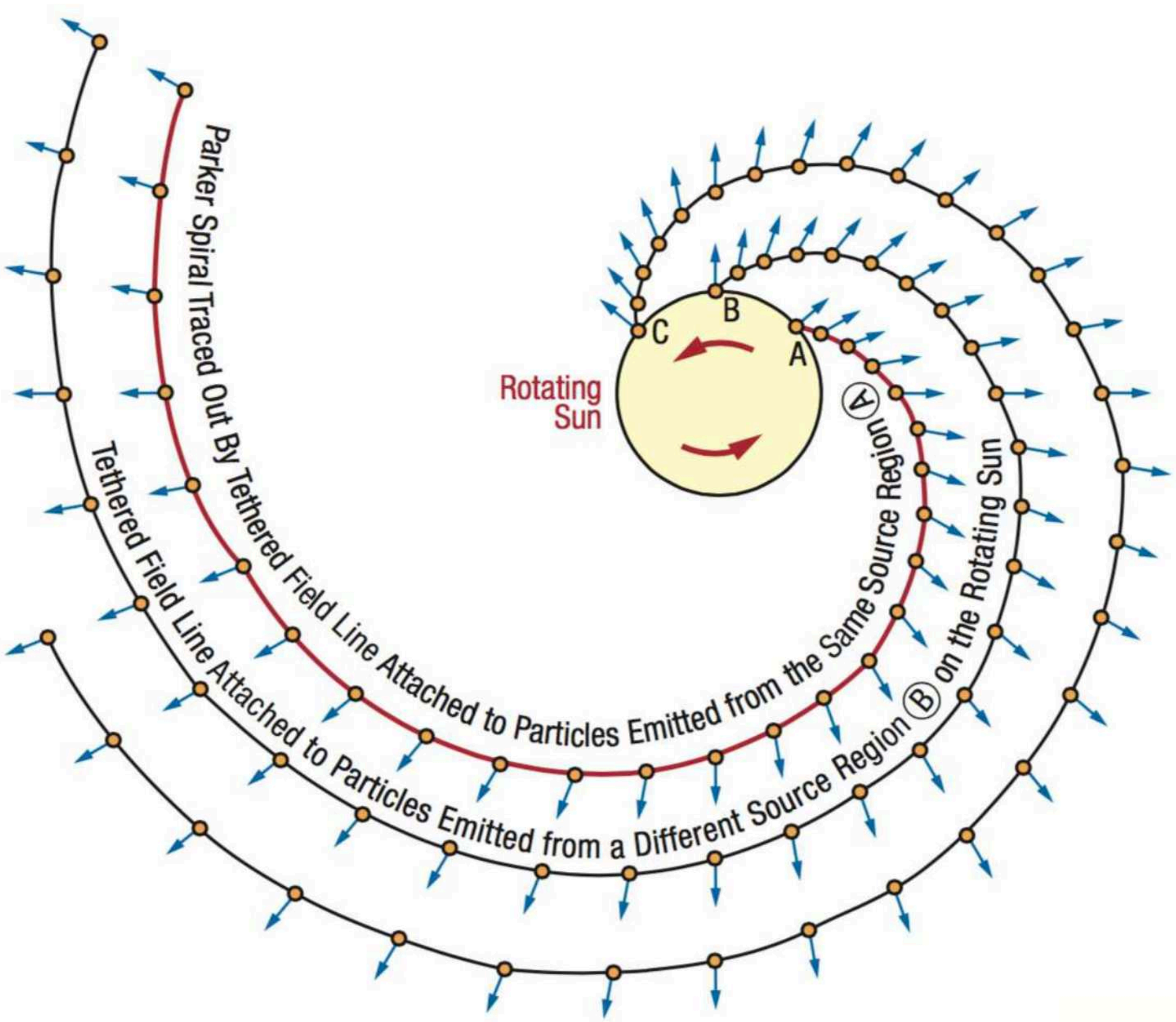

http://www.ieap.uni-kiel.de/et/people/heber/summerschoool/propagation.pdf

Heliospheric current sheet

https://en.wikipedia.org/wiki/Heliospheric_current_sheet

Photospheric Magnetic Maps

Observing *B* with Zeeman Effect

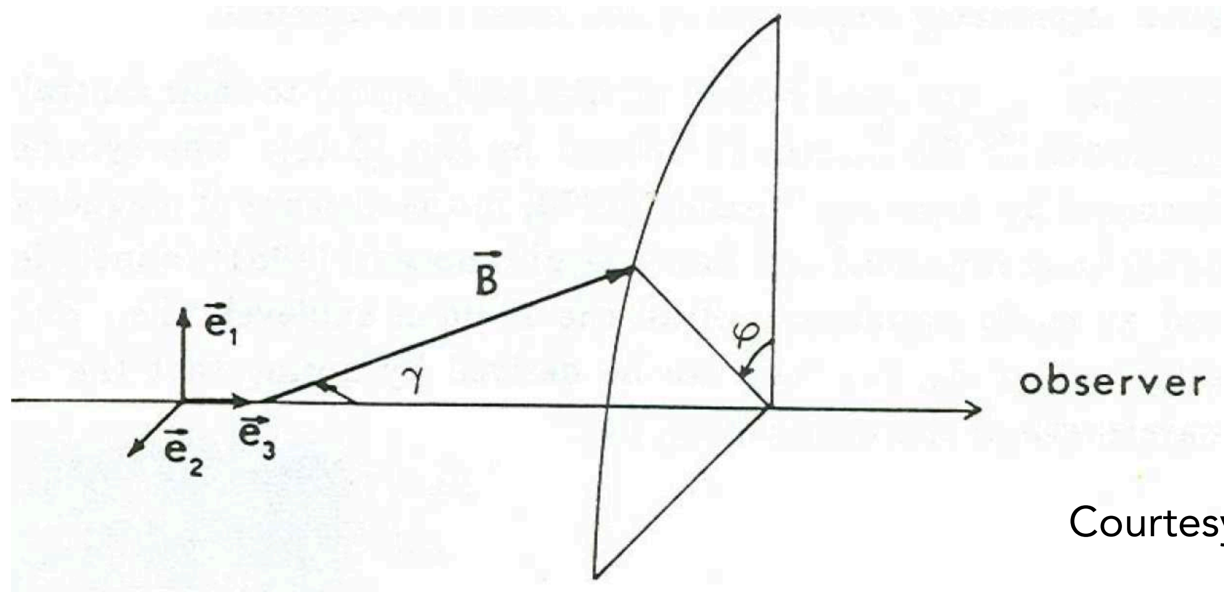

Courtesy J. Borrero

- For weak fields, Stokes profiles depend on field geometry

$$Q \propto B^2 \sin^2\gamma \cos 2\phi = B_t^2 \cos 2\phi$$
$$U \propto B^2 \sin^2\gamma \sin 2\phi = B_t^2 \sin 2\phi$$
$$V \propto B \cos\gamma = B_l$$

- Sensitivity of transverse field (***B****t*) is lower than longitudinal field (*B**l*)

$$\frac{Q}{I} < \frac{V}{I}$$

Longitudinal Magnetograms

WSO; Fe I 525.0/524.7 nm; 3′ resolution
22 × 11 pixels; 2 per day

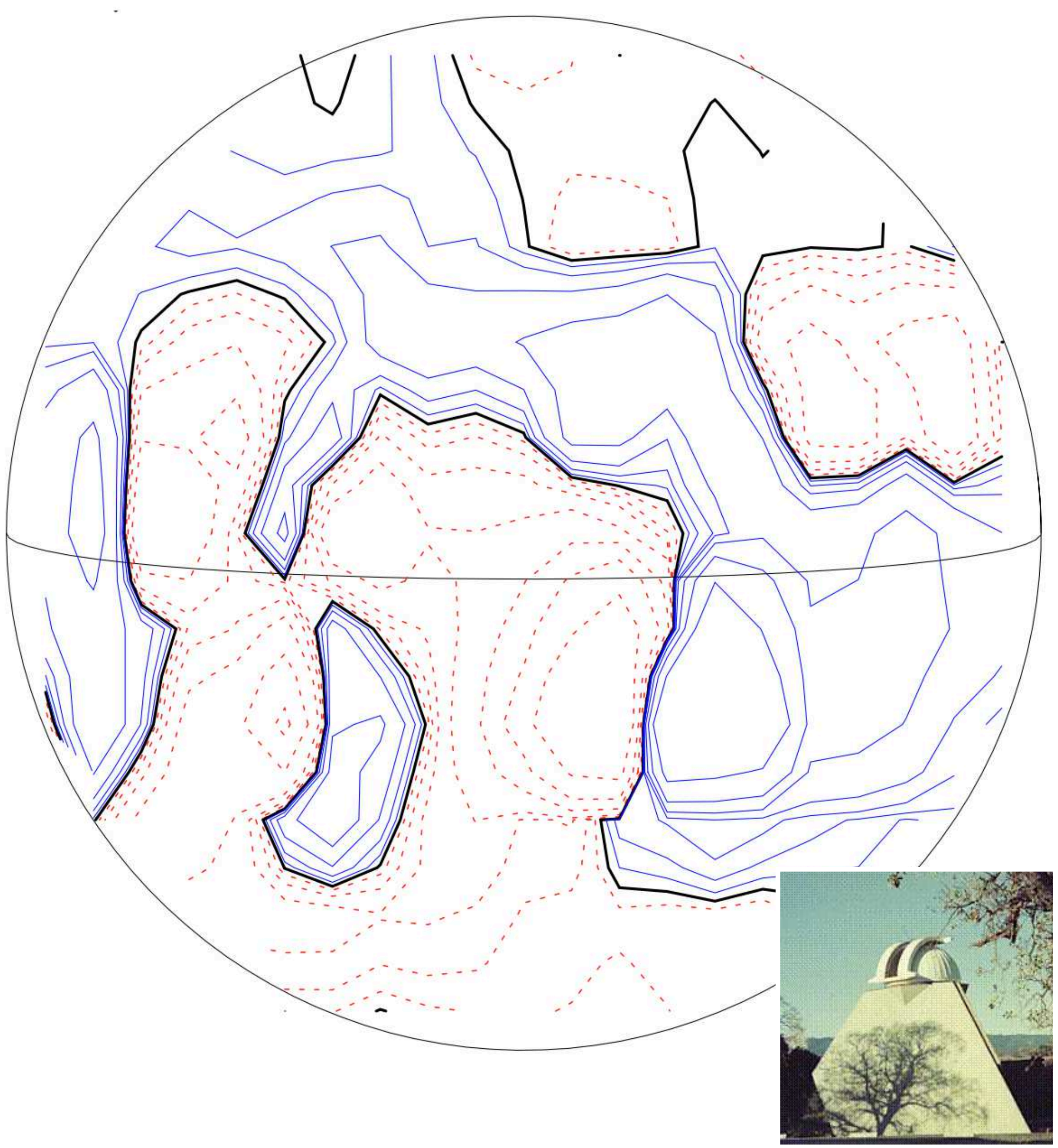

HMI; Fe I 617.3 nm; 1″ resolution
4096 × 4096; 1920 per day

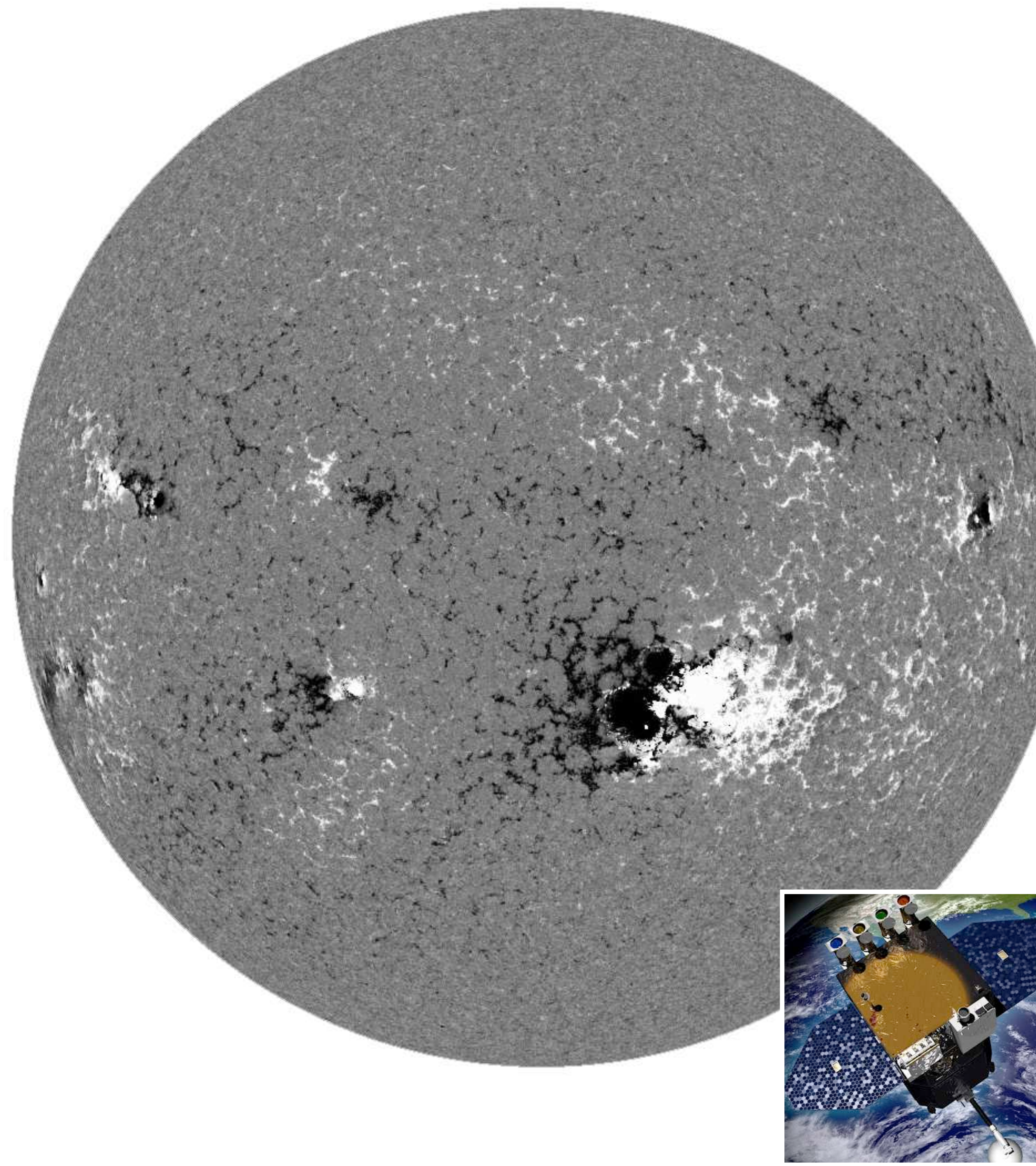

Synoptic Map

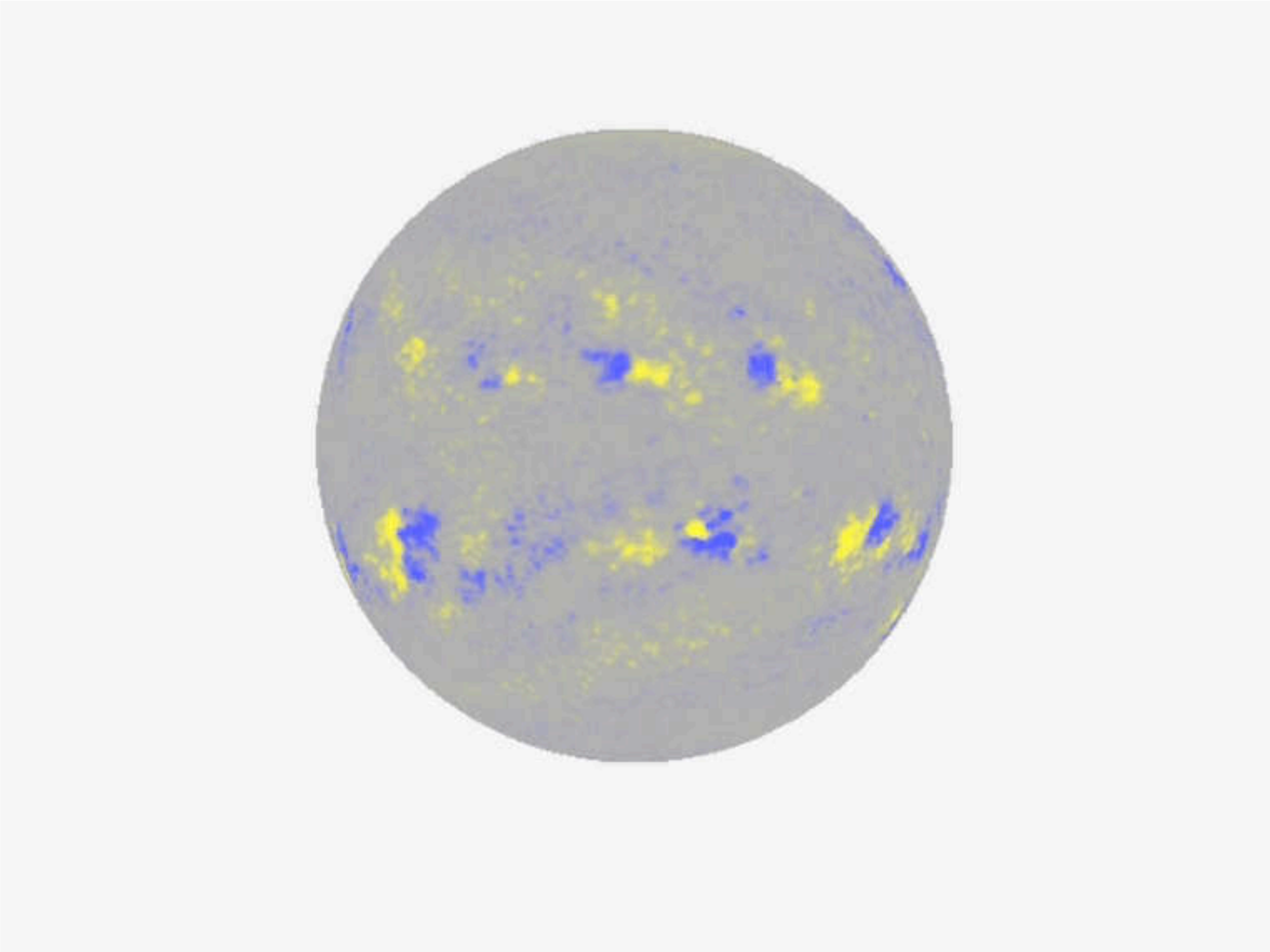

Hathaway (2015)

Synoptic Map & Heliographic Coord

$$B_r = B_l/\mu$$

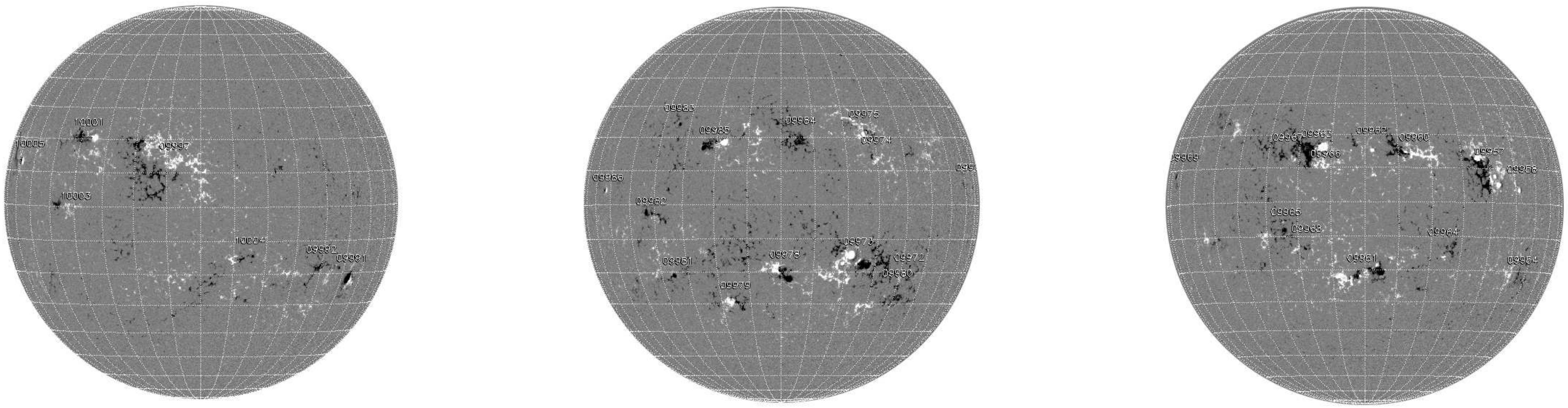

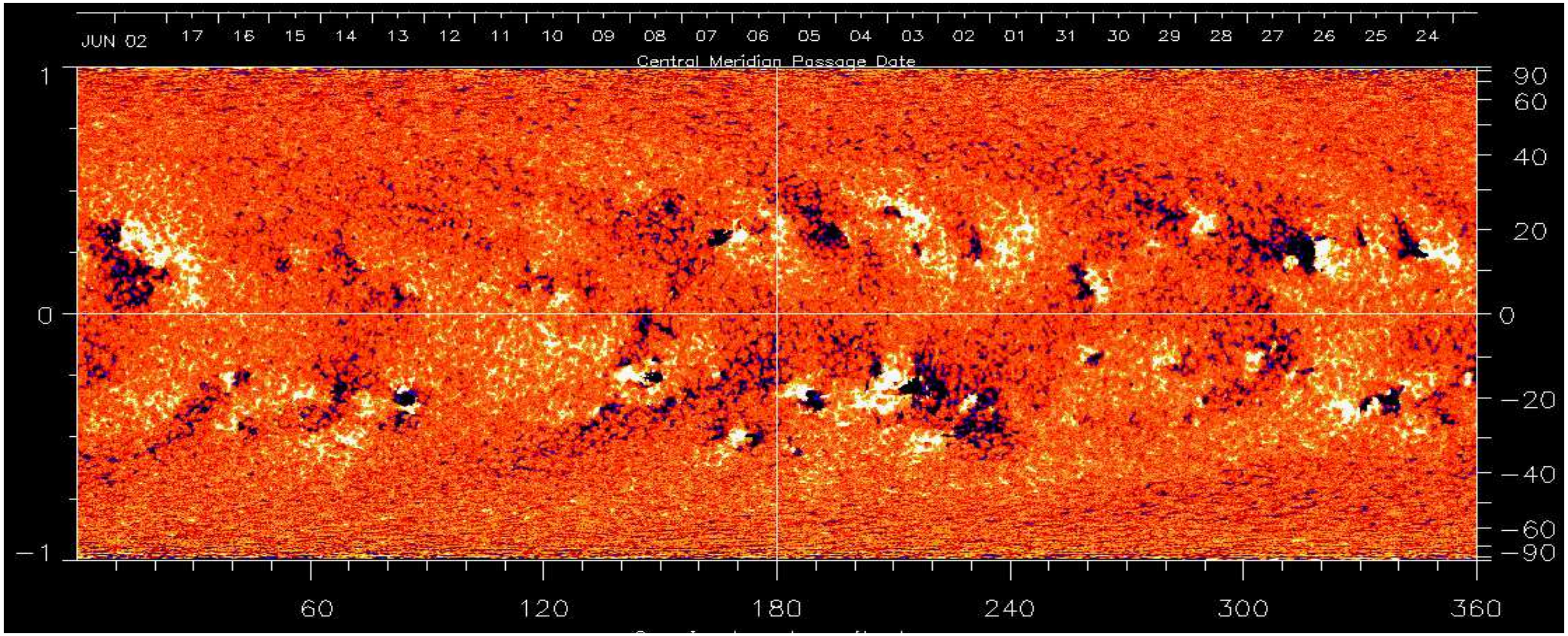

Nuisances

Synoptic

From Wikipedia, the free encyclopedia

Not to be confused with synopsis (disambiguation).

Synoptic is derived from the Greek words σύν (*syn*, "together") and ὄψις (*opsis*, "view"), and describes observations that give a broad view of a subject at a particular time. Specific uses include:

STEREO doesn’t have magnetograph…

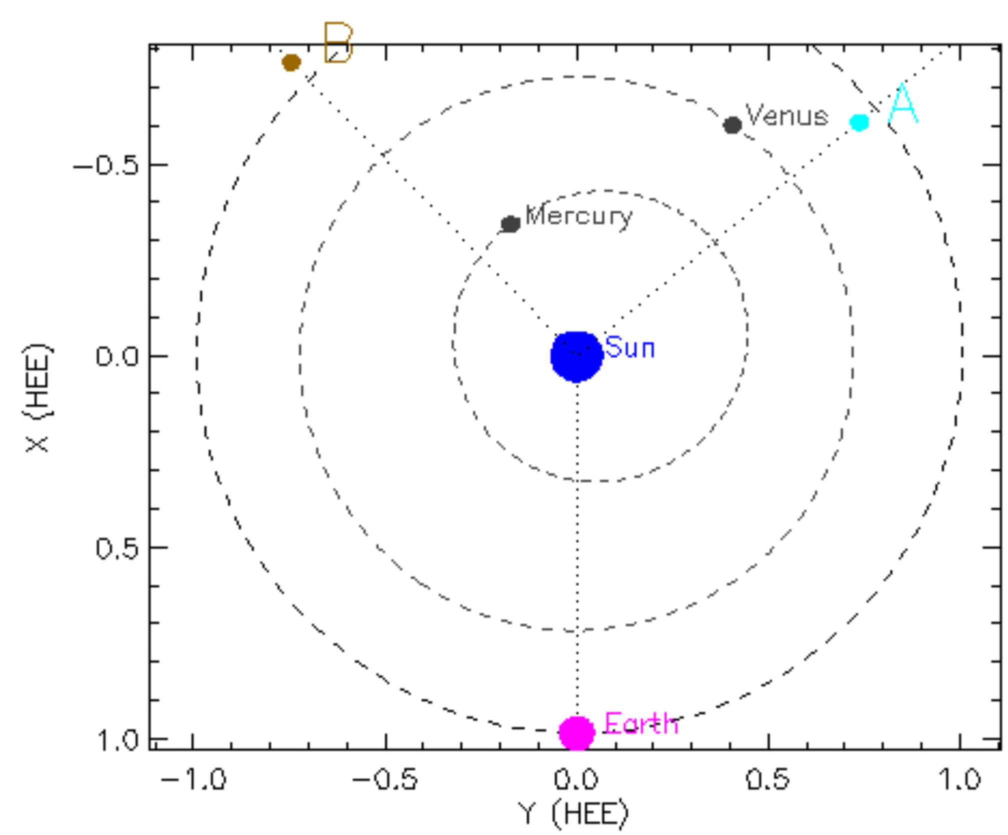

- Misnomer: not instantaneous snapshot
  - Different parts reflect conditions of different time
  - New emergence west of CMP not captured
  - Flux imbalance as half a bipole rotes on or off disc

Vector Magnetograms

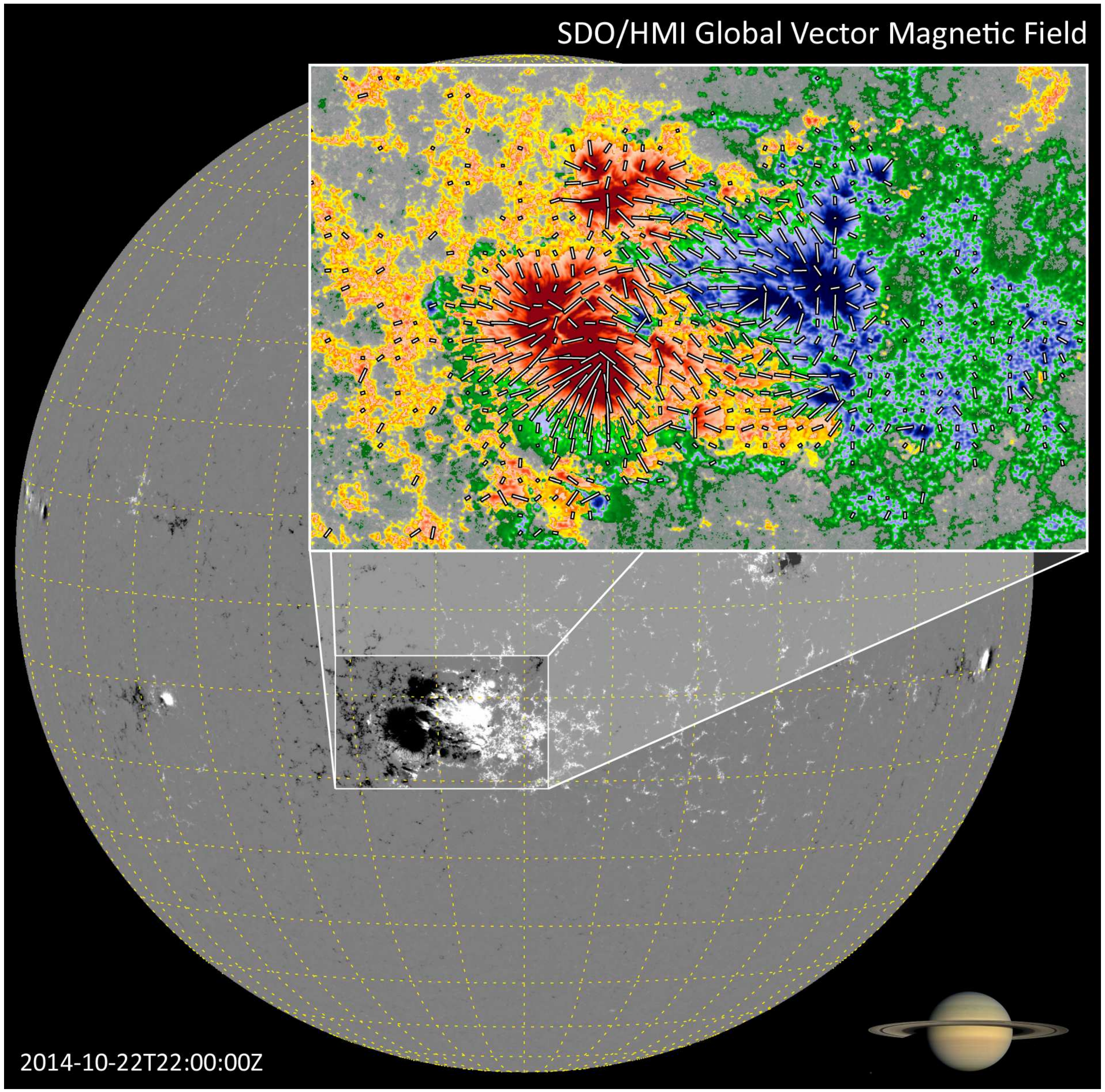

Choices, choices

- Cadence
- Field of view
- Duty cycle
- Spatial resolution
- ~~Spectral resolution~~

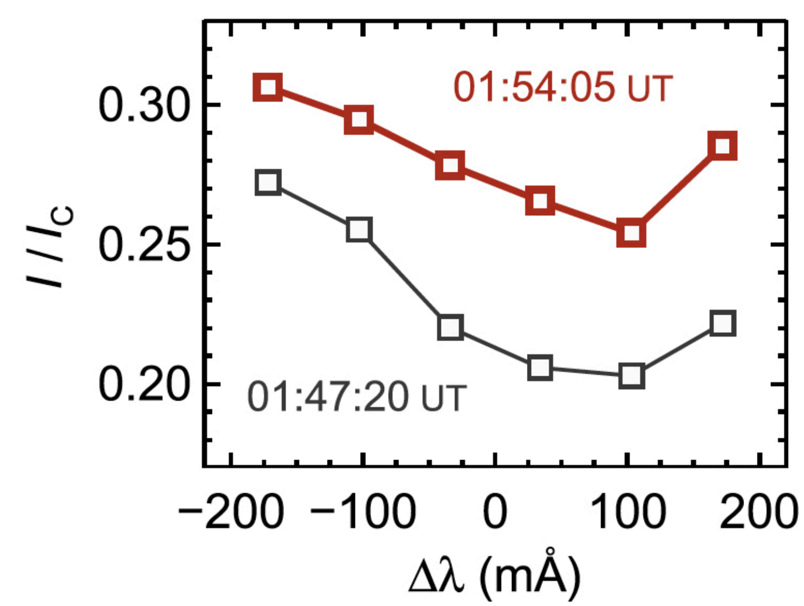

Azimuthal Ambiguity

- 180-deg azimuthal ambiguity inherent to Zeeman effect

$$Q \propto B_t^2 \cos 2\phi = B_t^2 (\cos^2 \phi - \sin^2 \phi)$$

$$U \propto B_t^2 \sin 2\phi = 2B_t^2 \sin \phi \cos \phi$$

- Requires additional model, e.g. minimizing "energy" (Metcalf 1996):

$$E = \sum (\lambda_1 |J_z| + \lambda_2 |\nabla \cdot \boldsymbol{B}|)$$

- Weak field azimuth is noisy

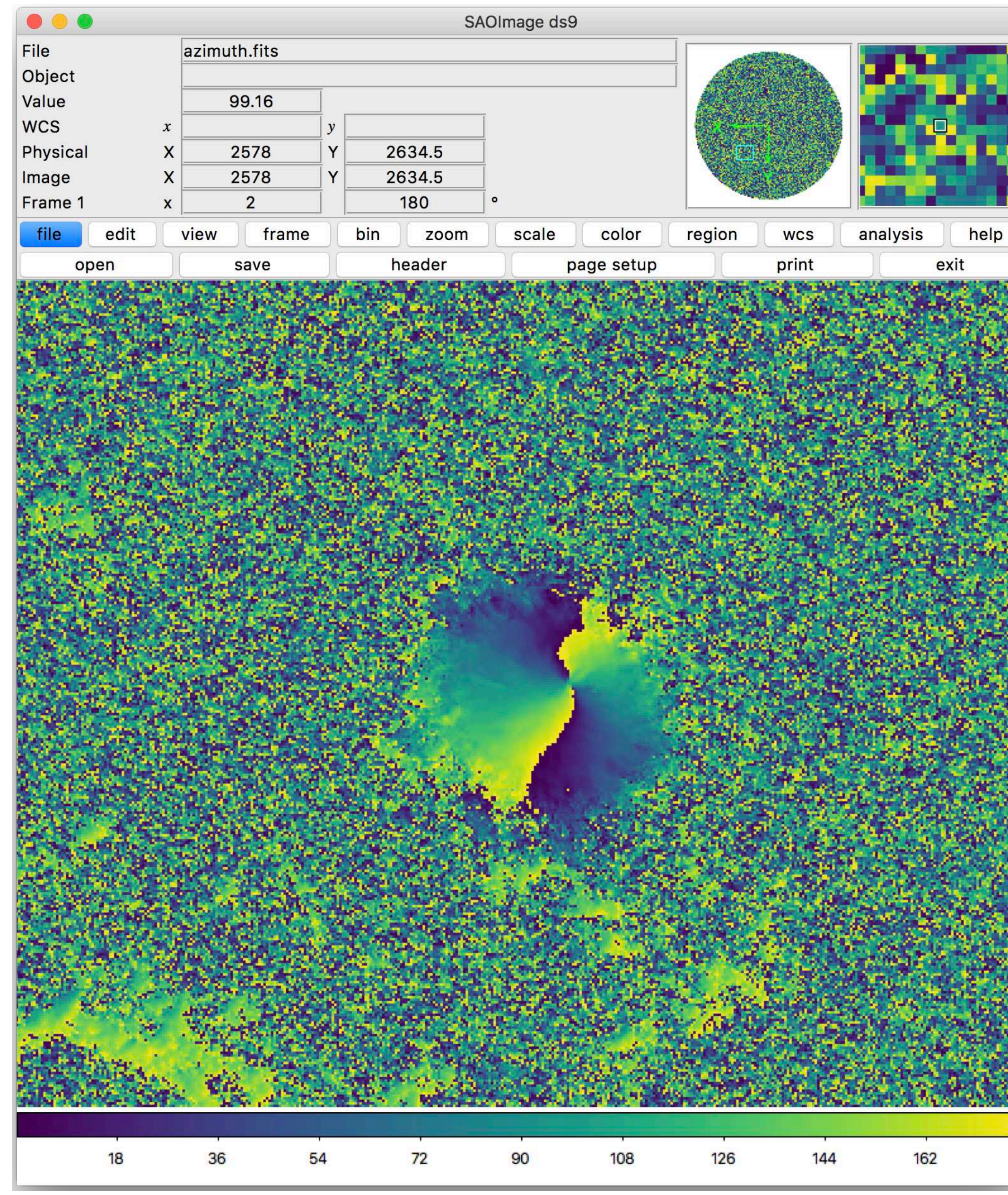

Vector Projection

- Inversion provides longitudinal field (*B_l*) from *V* & transverse field (***B_t***) from *Q*, *U*

- Usually we are more interested in radial (*B_r*) and horizontal (***B_h***) components

$$\begin{pmatrix} B_r \\ B_\theta \\ B_\phi \end{pmatrix} = \begin{pmatrix} k_{11} & k_{12} & k_{13} \\ k_{21} & k_{22} & k_{23} \\ k_{31} & k_{32} & k_{33} \end{pmatrix} \begin{pmatrix} B_\xi \\ B_\eta \\ B_\zeta \end{pmatrix},$$

- Relevant geometric parameters: *p*-angle, *b*-angle, longitude φ, latitude λ

- We are mixing signals with different noise characteristics (e.g., at poles)

$$k_{11} = \cos\lambda\,[\sin b \sin p \cos\phi + \cos p \sin\phi] - \sin\lambda\,[\cos b \sin p],$$
$$k_{12} = -\cos\lambda\,[\sin b \cos p \cos\phi - \sin p \sin\phi] + \sin\lambda\,[\cos b \cos p],$$
$$k_{13} = \cos\lambda \cos b \cos\phi + \sin\lambda \sin b,$$
$$k_{21} = \sin\lambda\,[\sin b \sin p \cos\phi + \cos p \sin\phi] + \cos\lambda\,[\cos b \sin p],$$
$$k_{22} = -\sin\lambda\,[\sin b \cos p \cos\phi - \sin p \sin\phi] - \cos\lambda\,[\cos b \cos p],$$
$$k_{23} = \sin\lambda \cos b \cos\phi - \cos\lambda \sin b,$$
$$k_{31} = -\sin b \sin p \sin\phi + \cos p \cos\phi,$$
$$k_{32} = \sin b \cos p \sin\phi + \sin p \cos\phi,$$
$$k_{33} = -\cos b \sin\phi.$$

Sun (2013)

The “Hedgehog”

HMI vector field sequence

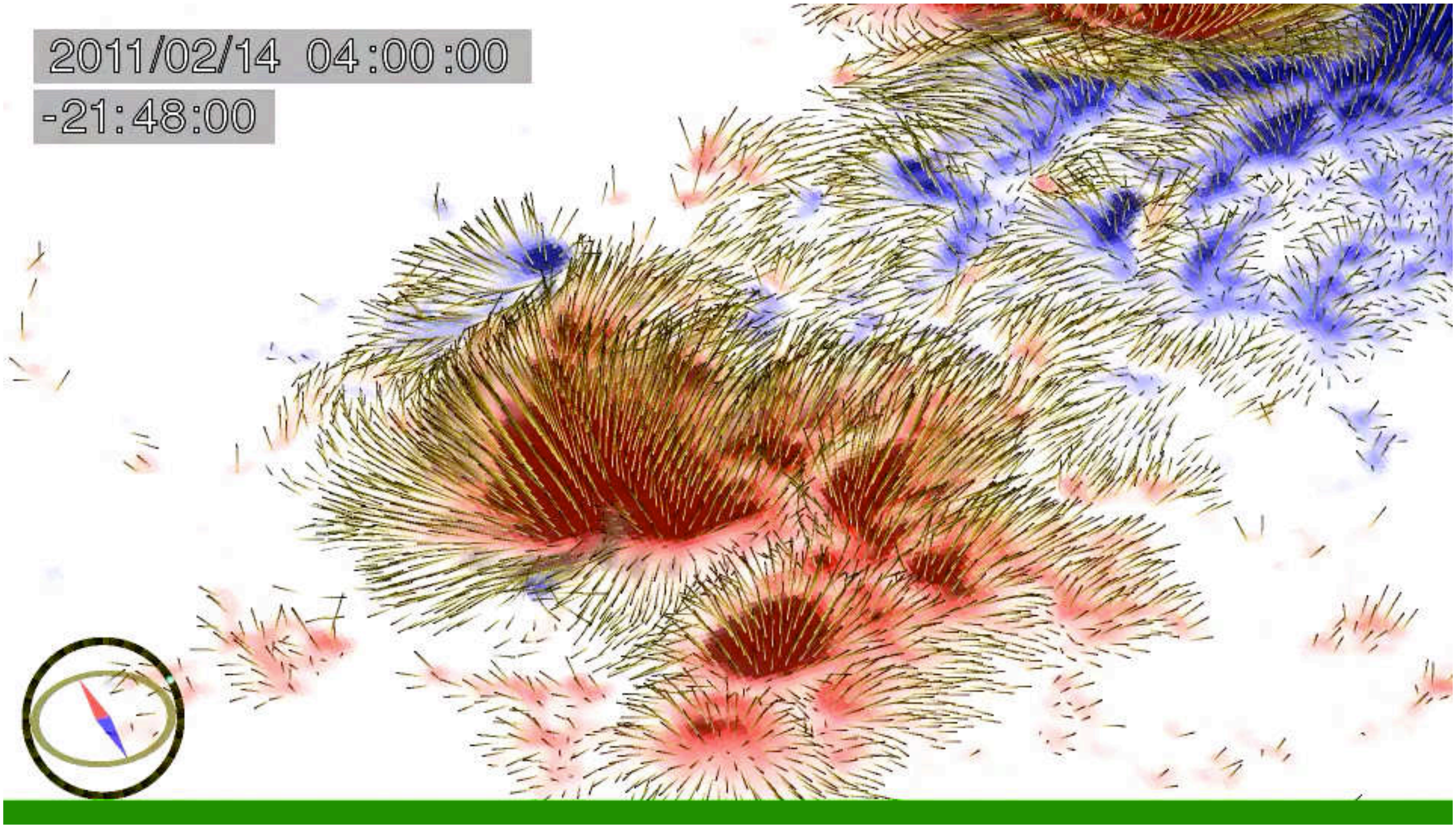

Courtesy K. Hayashi

More Nuisances

Rugged "formation" height

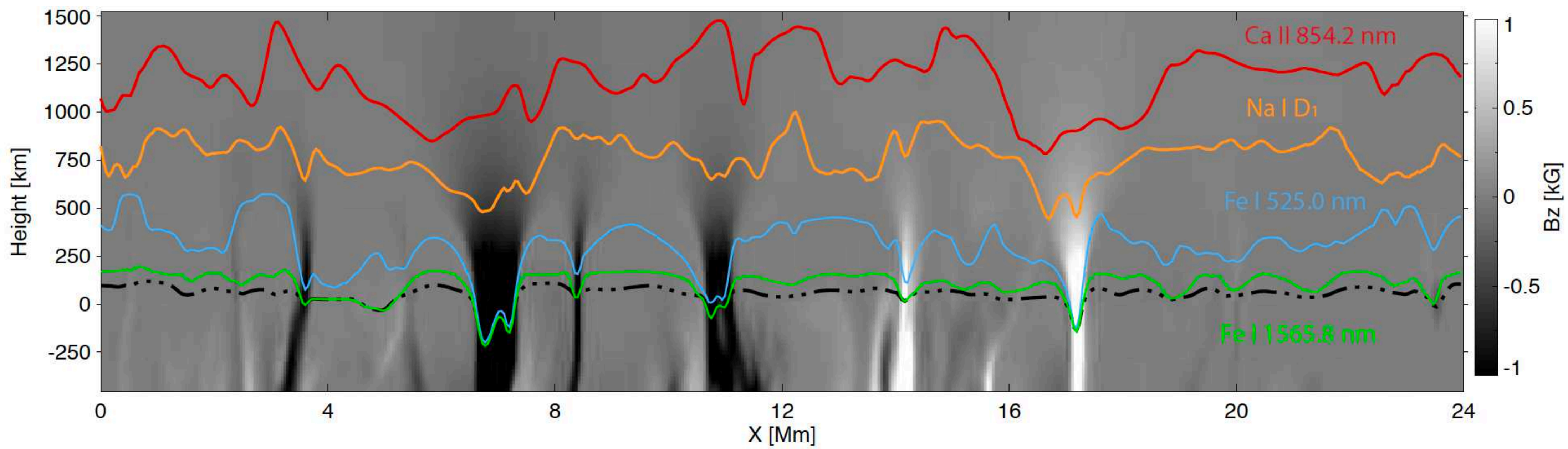

Courtesy C. Quintero Noda

Magnetic "filling factor"

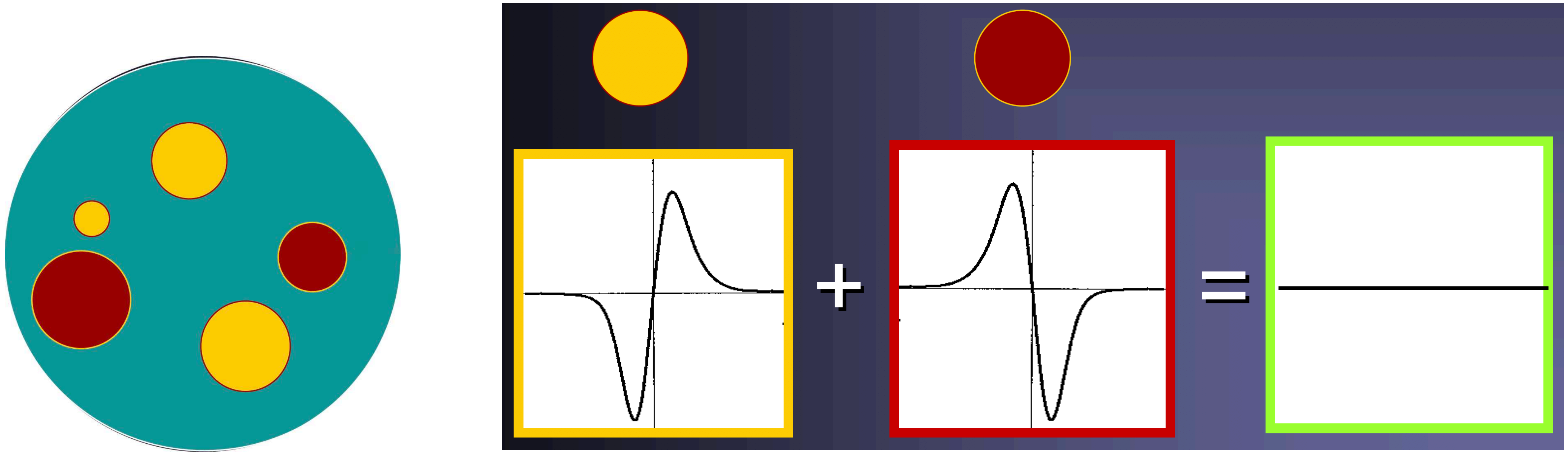

Courtesy S. Solanki

Potential Field of Quiescent Corona

Lorentz Force & Magnetic Pressure

- MHD momentum equation:

$$\rho \frac{d\boldsymbol{v}}{dt} = -\nabla p + \rho \boldsymbol{g} + \boldsymbol{j} \times \boldsymbol{B}$$

- Lorentz force: magnetic pressure gradient + tension force

$$\frac{1}{c}\boldsymbol{j} \times \boldsymbol{B} = \frac{1}{4\pi}(\nabla \times \boldsymbol{B}) \times \boldsymbol{B} = -\nabla \frac{B^2}{8\pi} + \frac{(\boldsymbol{B} \cdot \nabla)\boldsymbol{B}}{4\pi}$$

- Relative importance of plasma compared to field: plasma β

$$\beta = \frac{p}{p_{\rm mag}} = \frac{p}{B^2/(8\pi)}$$

Reign of Magnetic Field: Plasma β

$$\beta = \frac{p}{B^2/(8\pi)}$$

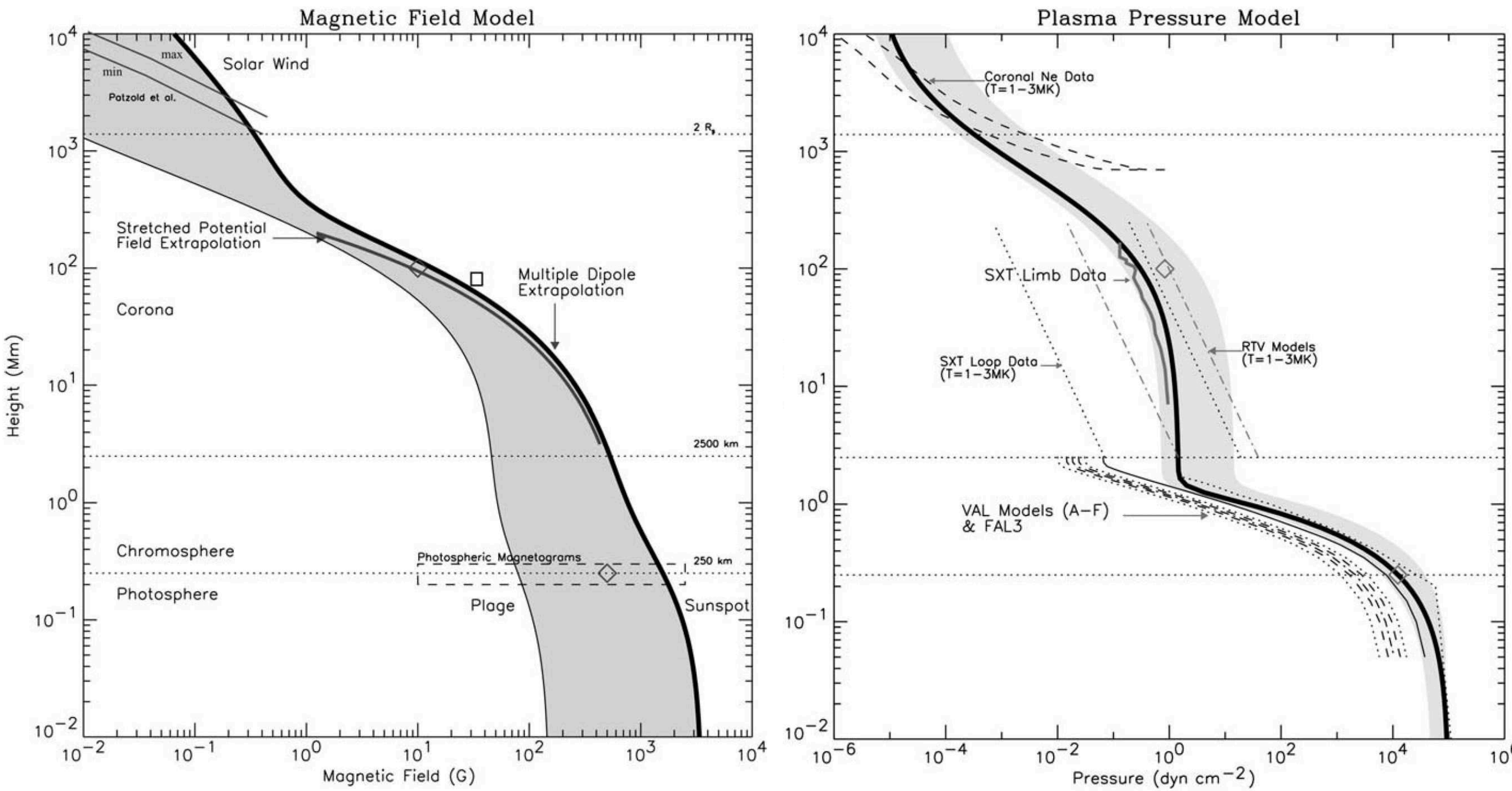

Gary (2001)

Plasma β & Force-Free Field

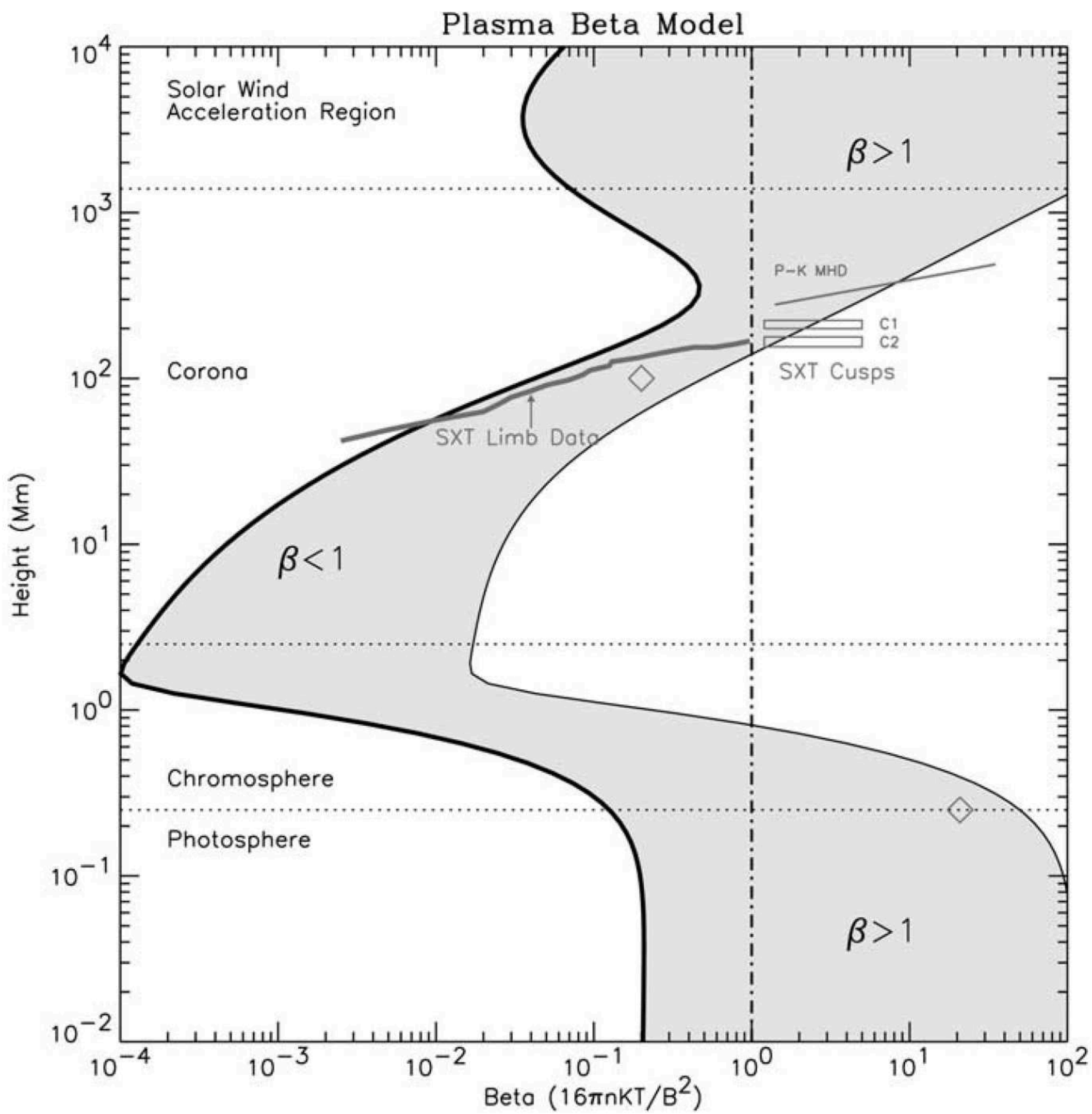

- Quasi-static (v ~ 0); low β

$$\boldsymbol{j} \times \boldsymbol{B} = 0$$

or

$$(\nabla \times \boldsymbol{B}) \times \boldsymbol{B} = 0$$

$$\nabla \times \boldsymbol{B} = \alpha \boldsymbol{B}$$

current (anti-)parallel to field

- Potential field α = 0; linear force-free field α is constant:

$$\nabla^2 \boldsymbol{B} + \alpha^2 \boldsymbol{B} = 0$$

- Lowest energy state

Gary (2001)

Electric Currents; Potential Field

- Electric currents exist as twist, shear, or discontinuity in ***B***

$$\int \boldsymbol{j} \cdot \mathrm{d}\boldsymbol{S} \propto \int \nabla \times \boldsymbol{B} \cdot \mathrm{d}\boldsymbol{S} = \oint \boldsymbol{B} \cdot \mathrm{d}\boldsymbol{l}$$

- Large-scale field is mostly current free, i.e. potential field (PF)

$$\nabla \times \boldsymbol{B}_p = 0$$

- Generally speaking, PF is the "lowest energy state"; "free" energy

$$E_f = \int \frac{B^2}{8\pi} - \frac{B_p^2}{8\pi} \mathrm{d}V$$

Where's ***j***?

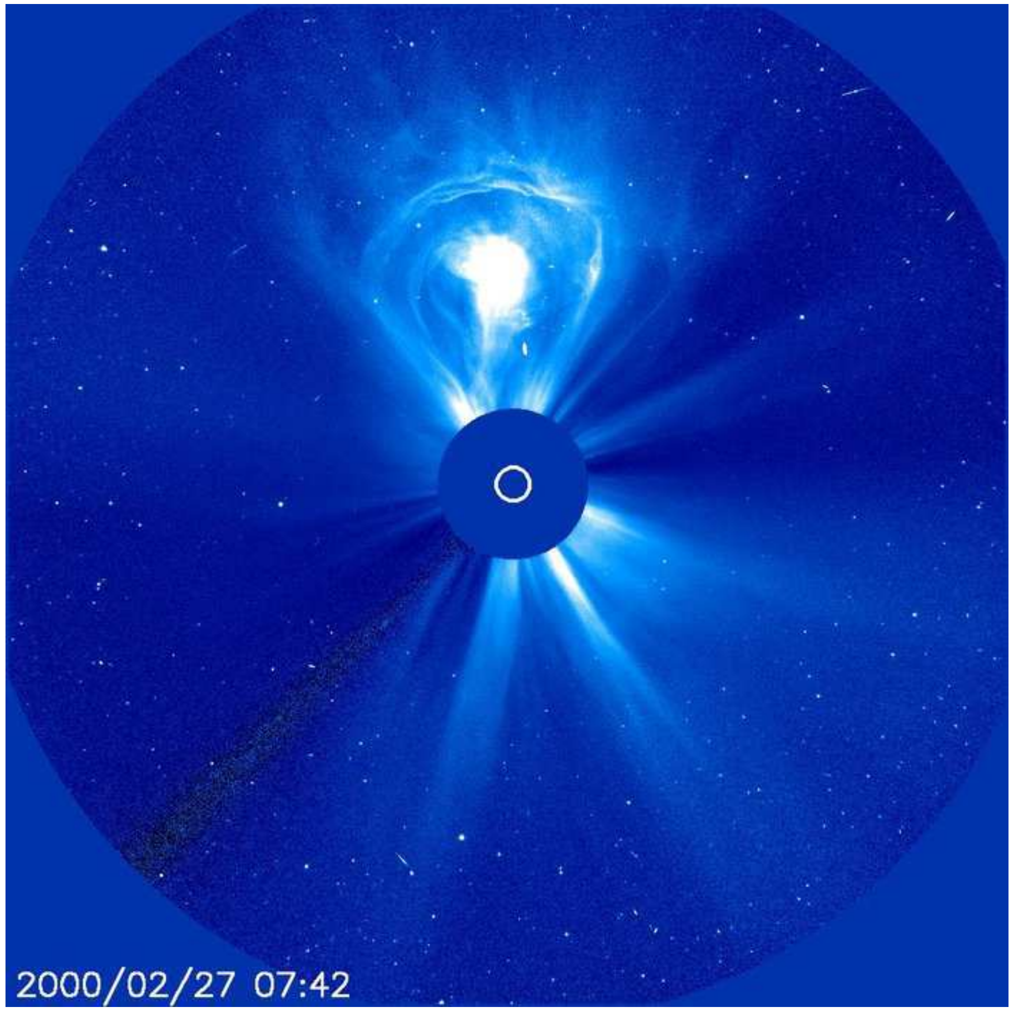

SoHO/EIT C3

PFSS Model

- Assuming lower corona is current free,
  B can be expressed as a scaler potential

$$\boldsymbol{B} = -\nabla\Psi$$

- ***B*** vector in spherical coord

$$B_r = -\frac{\partial\Psi}{\partial r}$$

$$B_\theta = -\frac{1}{r}\frac{\partial\Psi}{\partial\theta}$$

$$B_\phi = -\frac{1}{r\sin\theta}\frac{\partial\Psi}{\partial\phi}$$

- Coronal field governed by Laplace eq.

$$\nabla^2\Psi = 0$$

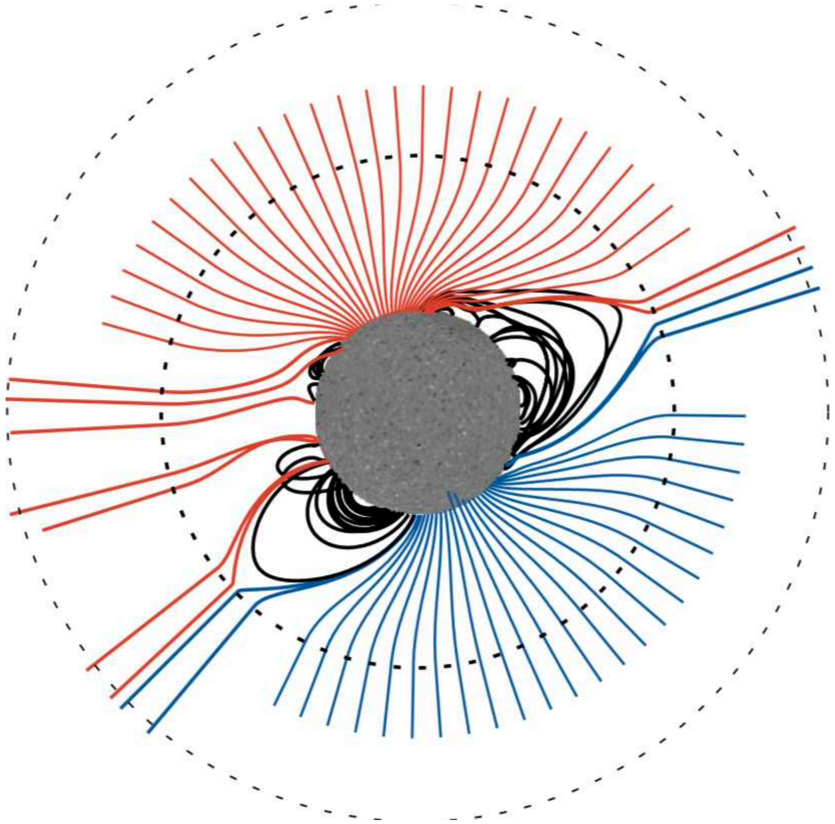

Sun (2012)

PFSS Model

- Inner boundary: photosphere radial field

$$-\left.\frac{\partial \Psi}{\partial r}\right|_{r=R_\odot} = B_r(\text{obs})$$

- Outer boundary: source surface where field becomes radial and open

$$\Psi\Big|_{r=R_s} = 0$$

$$R_s = 2.5R_\odot$$

- General solution of Laplace equation:

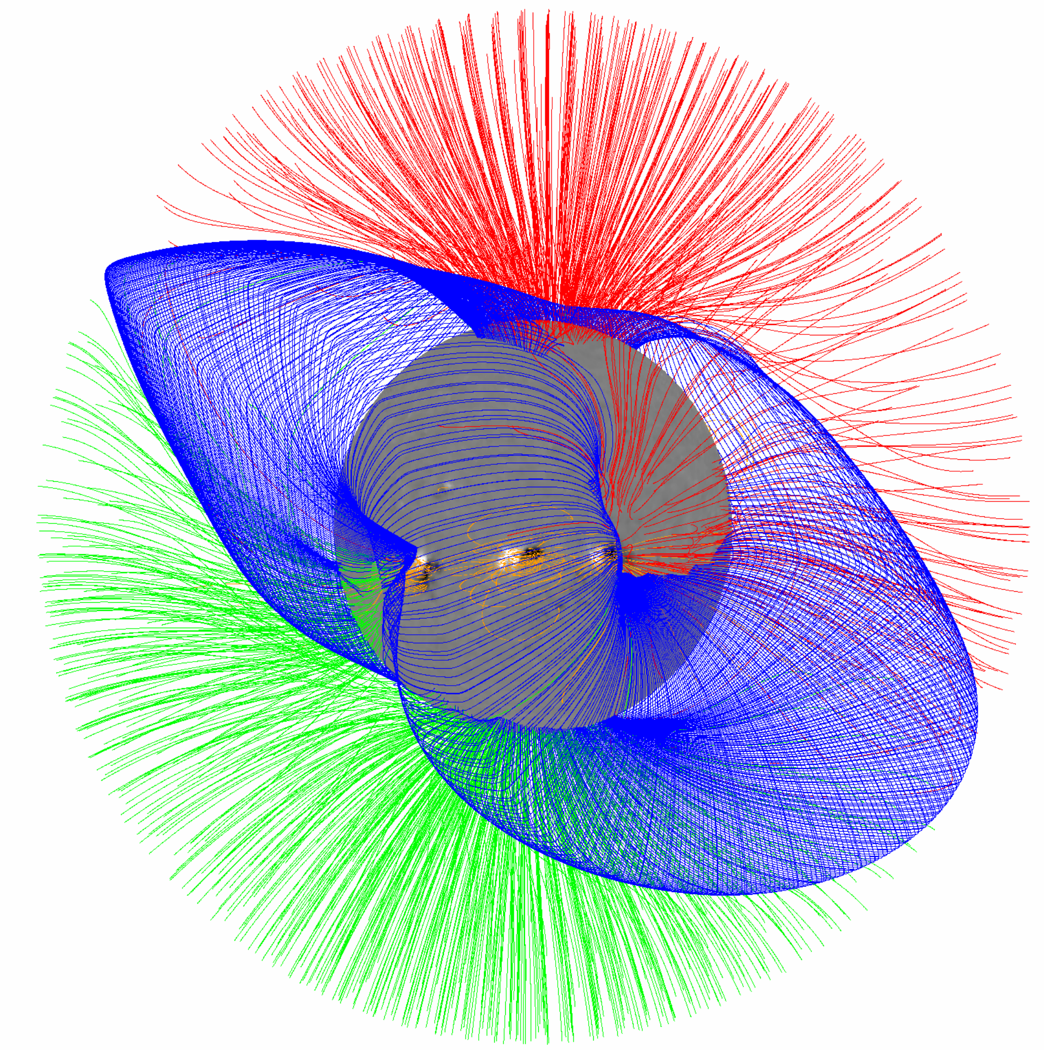

NSO/*GONG*

$$\Psi = \sum_{l=0}^{\infty} r^{-(l+1)} \sum_{m=-l}^{l} a_{lm} Y_l^m(\theta, \phi) + \sum_{l=0}^{\infty} r^l \sum_{m=-l}^{l} b_{lm} Y_l^m(\theta, \phi)$$

PFSS Model

- Coefficients can be obtained through spherical harmonics decomposition

$$k_{lm} \propto \int d\Omega \, Y_l^m(\theta, \phi) \; B_r \Big|_{r=R_\odot}$$

- Coefficients contain important information, e.g., dipole reverses sign

- Captures most topological features: current sheet location; streamer extent; coronal hole size/location

- Open field as solar wind sources

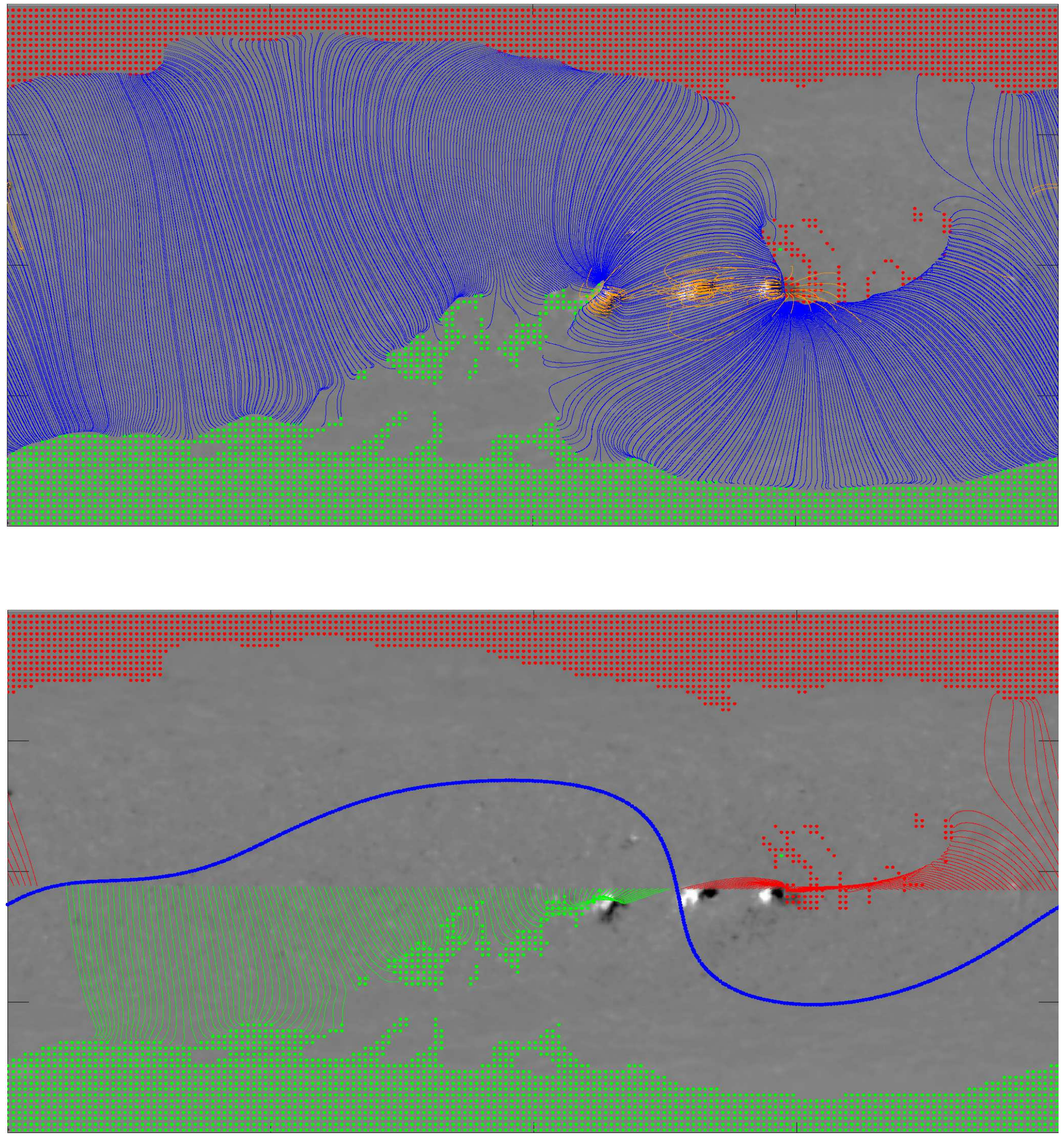

NSO/*GONG*

PFSS Widget

https://tinyurl.com/pfss-wid

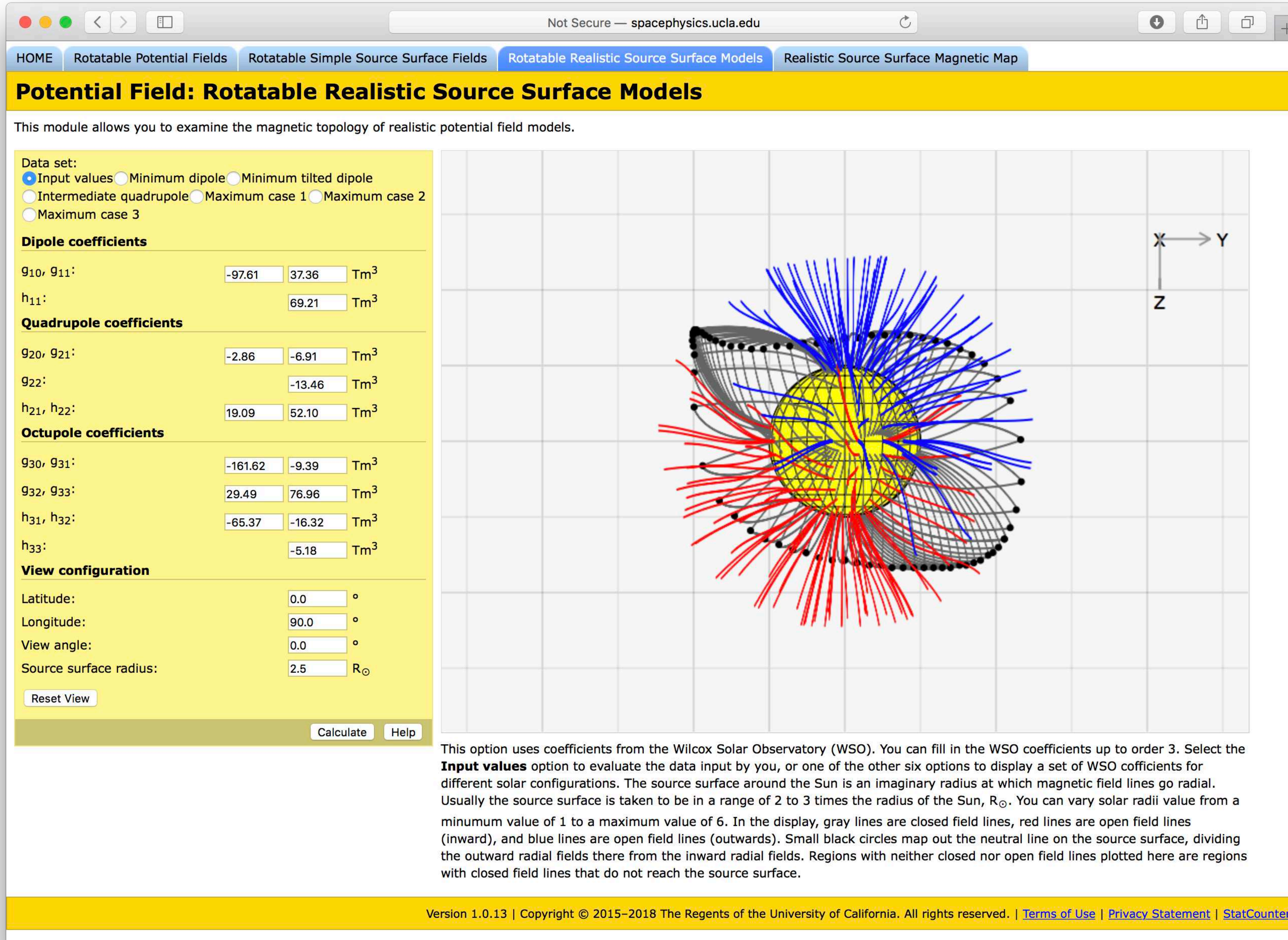

PFSS Model at Solar Min & Max

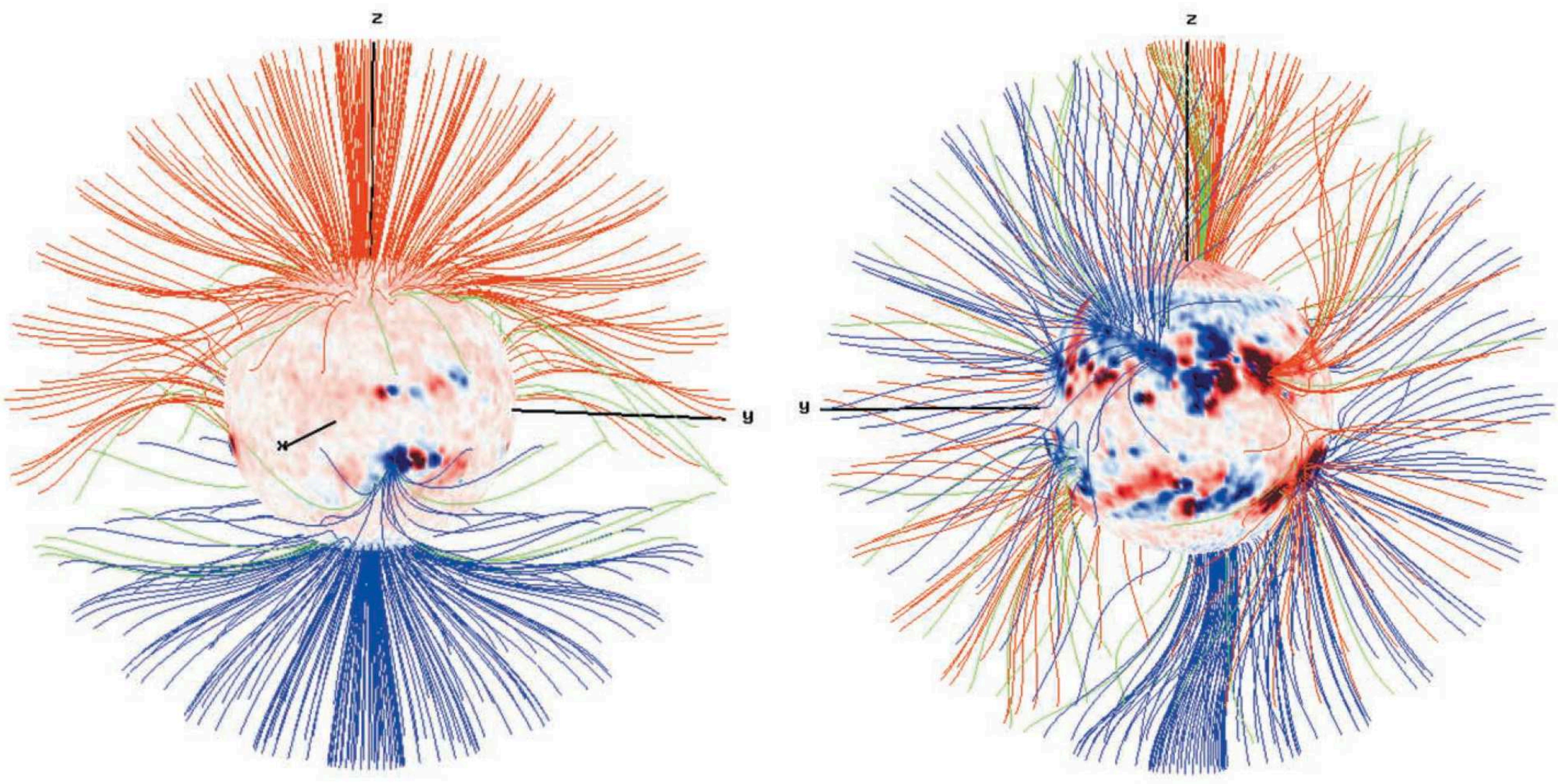

Neugebauer et al. (2002)